LA-4958

LA-4958

Detonations Near the Water Surface

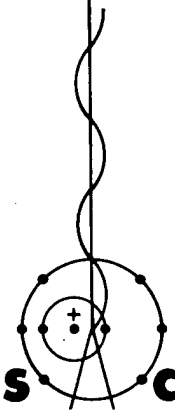

los alamos
scientific laboratory
of the University of California
LOS ALAMOS, NEW MEXICO 87544

UNITED STATES
ATOMIC ENERGY COMMISSION
CONTRACT W-7405-ENG. 36

Printed in the United States of America. Available from
National Technical Information Service
U. S. Department of Commerce
5285 Port Royal Road
Springfield, Virginia 22151
Price: Printed Copy $3.00; Microfiche $0.95

LA-4958
UC-34
ISSUED: June 1972

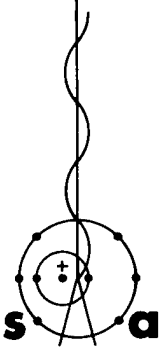

los alamos
scientific laboratory
of the University of California
LOS ALAMOS, NEW MEXICO 87544

Detonations Near the Water Surface

by

Charles L. Mader

DETONATIONS NEAR THE WATER SURFACE

by

Charles L. Mader

ABSTRACT

The results of an experimental and theoretical study of the compressible flow resulting from a sphere of 9404 explosive initiated at its center and partially immersed in water are described. The flow was studied experimentally using radiographic and photographic techniques. Compressible hydrodynamic calculations were performed using multicomponent Eulerian numerical techniques.

I. INTRODUCTION

The prediction of water waves generated by large-yield explosions has been based on extrapolation of empirical correlations of small-yield experimental data. The accuracy of such predictions is unknown so there is a need for a detailed description of the mechanism by which waves are generated by explosions. The effect of detonation depth needs to be better understood. The "upper critical depth," i.e., the depth at which a peak of the wave amplitude occurs, is not understood. The effects near the explosion when the flow is quite compressible, such as surge, shock wave propagation, separation of the shock wave from the bubble, and the wave pattern near the explosion have previously received little theoretical or experimental attention in the region of the upper critical depth.

This is a progress report of a study of the early interaction of the detonation products with the water and air interfaces and the resulting wave profile near the detonation. The initial phase of this study was described in Ref. 1.

To determine if compressible hydrodynamic calculations were feasible, given the techniques developed during the last 15 years for describing detonation phenomenon and equations of state, the early time behavior of the diverging detonation was calculated and compared with experimental radiographic results. The calculated results were also compared with detailed early time measurements of the shock wave in water produced by a diverging detonation and with late time measurements where the interaction of the detonation products and the water was followed for at least one complete oscillation of the bubble. The observed agreement between the observed short- and long-time behavior of an underwater detonation and the detailed one-dimensional compressible hydrodynamic calculations suggests that the calculated energy partition between detonation products and the water is sufficiently accurate to be used in multidimensional studies of wave-generation mechanisms.

II. PHERMEX EXPERIMENTAL RESULTS

The Los Alamos Laboratory radiographic facility PHERMEX[2] (Pulsed High Energy Radiographic Machine Emitting X-Rays) is a radiographic facility which produces an x-ray pulse by impinging 27-MeV electrons, generated by a standing wave linear accelerator, upon a 0.7-mm diam. tungsten target. Radiation intensities of 5.0 R are obtained at the experimental system being studied (positioned approximately 3 m from the target). An x-ray film is placed approximately 0.75 m behind the experimental system in a protective aluminum case. This arrangement gives radiographic resolution of ± 0.1 μsec and ± .02 cm without time smear.

A sphere of explosive consisting of a 0.635-cm radius PETN (Estex XTX8003, 80/20 by wt. PETN/silicone binder) and 0.635 cm of 9404 was detonated at the center. The sphere was placed half in the water in the radiographs taken at 15.8 and 26.3 μsec after detonation was initiated. The detonation wave arrived at the explosive surface in 1.5 μsec. The sphere was placed two-thirds in the water in the radiograph taken at 61.3 μsec. The position of the water-detonation product interface, the splash wave and the water shock wave may be determined from the radiographs. The static and dynamic radiographs and sketches of the prominent features of the radiographs are shown in Figs. 1, 2, and 3.

One-dimensional SIN calculations similar to those described in Ref. 1 were performed for the explosive sphere in water at one atmosphere density and in air at one Los Alamos atmosphere. The water equation-of-state parameters used were identical to those described in Ref. 1. The equation-of-state parameters used for 9404, PETN, and air are given in Table I. The position of the water shock and bubble radius as a function of time are shown in Fig. 4. Also shown are the positions found in the radiographic study shown in Figs. 1, 2, and 3. The calculated pressure of the water shock and the 9404-water interface are shown in Fig. 5. The position of the air shock and the 9404-air interface as a function of time is shown in Fig. 6. The calculated pressure of the air shock and the 9404-air interface as a function of time is shown in Fig. 7. Since the position of the water-detonation product interface and the water shock wave along the vertical axis in the radiographs is in good agreement with the one-dimensional calculations, we used the results of the one-dimensional calculations to obtain estimates of the pressures in the water and the positions of the air shock, air-detonation product interface, and the pressures along the vertical axis at the times of the radiographs. The results of this exercise are sketched in Fig. 8.

TABLE I

HOM EQUATION OF STATE CONSTANTS

	PETN	9404	AIR (0.76 Bar)
A	-3.10639868833 +00	-2.88303447687 +00	-2.36733372864 +00
B	-2.25210297095 +00	-2.25910150671 +00	-1.23356432554 +00
C	+1.93865645401 -01	+2.09836811364 -01	+2.15170143603 -02
D	+1.06761114309 -02	-1.62402872478 -02	-2.95528542190 +03
E	-5.71317097698 -05	+4.14247701072 -04	+1.22549782442445-04
K	-1.43880401718 +00	-1.27244575845 +00	-5.53376189904 -01
L	+4.17630232758 -01	+4.27159472916 -01	+2.44880013455 -03
M	+4.43146793248 -02	+4.61539702874 -02	+1.80516553555 -02
N	+2.43302842995 -03	+2.54544398316 -03	-1.219686716B8 -03
O	+5.15057824089 -05	+5.31474988838 -05	-2.53726183472 -05
Q	+8.10009012302 +00	+8.24707528084 +00	+9.88588851357 +00
R	-3.67433055630 -01	-4.89534325865 -01	-2.35014643148 -01
S	+1.38196579791 -03	+6.12169699021 -02	+3.36987666054 -02
T	+8.14028829459 -03	-3.22067926443 -03	-4.21156020156 -03
U	-7.34294504930 -04	-5.13495324073 -06	+1.63045512702 -04
C_V^*	+0.5	+0.5	+0.5
Z	+0.1	+0.1	+0.1
P_o	+1.55 g/cm^3	+1.844	+0.00107567
P_{CJ}	+0.231 mbar	0.363	
D	+0.740 cm/μsec	0.8880	
T_{CJ}	+3369 °K	2460	
P_{Max}	+0.40	+0.40	+1.0 -03
P_{Min}	+1.0 -08	+1.0 -08	+1.0 -08
Isentrope Pressure	0.40	0.40	5.0 -04

III. PHOTOGRAPHIC EXPERIMENTAL RESULTS

The experimental arrangement is sketched in Fig. 9. Three cameras, a 1-sh flash, a GMX-8 rotating-mirror camera, and an optical arrangement that gave an 18-in. diam field of parallel light, were used to make a high-resolution shadowgraph of the gas bubble 302 μsec after the load ring pulse. A wax shutter was used to prevent overwrite. The time was chosen so that the surface-wave tip, if resolved, would be within the field. The wave tip was obscured by detonation products but the gas bubble (products/water) interface was clearly resolved. The bubble radius was 8.03 cm. Another camera, the GMX-6 Dynafax framing camera, viewed a 36-in. by 36-in. field, half of which was below water level. Back lighting for this camera was accomplished with the GMX-2 electronic xenon flash unit and a diffuser screen made from Mylar drafting paper. The camera was operated at 2151 rps so that the nominal time between frames was 29 μsec; exposure time was 1 μsec per frame. The third camera was a Bolex H-16 Reflex cine camera with a framing rate of 64 frames per second and exposures times of 0.002 sec per frame. Quantitative data obtained from the first two cameras are plotted in Fig. 10. Also shown are the results of one-dimensional SIN hydrodynamic calculations for the explosive system immersed in water at 1 bar. The deviation becomes significant after 100 μsec. Two-dimensional hydrodynamic calculations will obviously be required to describe the flow at later times.

The results from the cine camera are shown in Figs. 11 and 12. Since these data are affected by bottom and side effects in the geometry used, additional experiments in a larger tank will be required to determine the magnitude of such effects.

IV. TWO DIMENSIONAL COMPRESSIBLE HYDRODYNAMIC CALCULATIONS

The EIC code,[3] which uses the Particle-In-Cell (PIC) method, was used to study the dynamics of a sphere of 9404 detonated at the water surface. Particle plots are shown in Fig. 13. The calculated position along the vertical axis was in agreement with the SIN one-dimensional calculations described previously. The splash wave was not as large or as high as observed and the detonation products and air shock did not travel as far as predicted by the SIN calculations. Since the resolution available from a PIC calculation is severely limited, such disagreement may be expected. The calculations did indicate that larger splash waves occur with time and increasing water depth.

The 2DE code[4] has recently been developed to calculate multicomponent reactive hydrodynamic problems in slab or cylindrical geometry using continuous Eulerian equations of motion. Numerical solutions of severely distorted flow problems, such as the interaction of shocks with V notches, cylindrical voids, and aluminum rods in water, have given results that closely reproduced those observed experimentally.[5] The high resolution available with the technique makes it attractive for problems with large distortions such as the problem of the explosive sphere interacting with a water surface. The present code gives accurate solutions for mixed cells with two components, but approximations are necessary if three or more components are present in a cell. Since the splash wave results in cells of water, detonation products and air, the region of the splash wave is not as accurately defined as the rest of the flow.

One-dimensional SIN calculations indicated that the results of the calculation were only slightly changed if the PETN-9404 explosive sphere was replaced by an all 9404 explosive sphere with the inner 0.4-cm radius initially detonated at constant volume. The larger "initiator" was necessary in the two dimensional calculations because of the large cell size used for economy reasons.

The 2DE calculations were performed with a mesh of 100 cells in the Z direction and 50 or 100 cells in the R direction. Several cell sizes were tried. The largest cell size that would give results independent of the mesh size was 0.0635 cm, which gave 20 cells along the radius of the explosive sphere. Smaller cell size would be required for definition of the splash wave; however, a more exact treatment of the three component cells would be necessary before such calculations could be justified. A smaller cell size would also permit a better description of the air shock and the 9404-air interface.

Calculations were performed for the 9404 sphere completely immersed under 1.27 cm of water. The isoplots of the calculated flow are shown in Fig. 14. Calculations were performed for the 9404 0.625 immersed in water. The isoplots of the calculated flow are shown in Fig. 15.

A comparison of the 2DE calculated position of the water shock, 9404-water interface, and the water shock pressure as a function of time, and the one-dimensional SIN results are shown in Fig. 16. A similar comparison for the air shock and 9404-air interface is shown in Fig. 17. The 2DE calculation did not resolve the position of the air shock. Agreement between the various calculations is necessary during the early part of the flow if the calculations are accurate. The agreement is remarkable and suggests that the 2DE calculations may be trusted within the numerical resolution.

V. DISCUSSION

In his studies of the underwater explosion pulsation problem, Pritchett[6,7] has demonstrated that theoretical results that include the effect of compressibility tend to agree with the incompressible water calculations. Since the calculations described in this report and in Ref. 1 show that the flow is determined by the impulse and resulting momentum imparted to the water by the time the shock wave in the water has traveled three to five radii of the initial explosive, it is clear that, if the initial impulse assumed by the incompressible calculation is approximately correct, the remainder of the flow should be accurately described by the incompressible assumption. These results suggest that we have already solved the compressible flow problem for a sufficient interval to give us a good first approximation of the initial conditions to use in an incompressible calculation. Further numerical studies should probably be performed with either a good incompressible technique that accurately

describes the surface boundary or an almost incompressible technique such as ICE.[8]

As mentioned in the introduction, we are interested in the region of the upper critical depth. The upper critical depth has been elegantly reviewed by Le Mehaute.[9] In regard to this phenomena, the calculations show that the water in and near the splash wave has a large amount of momentum. In particular, as shown in Fig. 17, the velocity in the radial direction is up to 5 times larger in the water near the splash wave than in the rest of the shocked water. This concentration of momentum near the water surface could be a contributing factor to the phenomenon of upper critical depth. Whether or not it is important for the late-time wave behavior, it is the reason that the observed horizontal bubble radius is larger than the vertical bubble radius for explosions near the water surface, as shown in Figs. 4 and 10.

The high velocity present in the splash wave is a result of the initial water shock being quickly rarefied and permitting a second shock to be delivered from the explosive products. Subsequent shocks and rarefactions occur while the detonation products still have high pressures. Each reverberation increases the particle velocity of the splash wave by an increment that decreases as the pressure of the driving detonation products decreases. The particle velocity of the remainder of the water cannot be increased by reverberations during the early high-pressure motion since a free interface is not available.

The estimated period of a 1.27-cm radius 9404 sphere immersed in water at 1 bar pressure is 0.1 sec and the maximum bubble radius is 44.2 cms. As shown in Fig. 12, the observed maximum radius is slightly larger and the period is 4 to 5 times larger than the estimated radius and period. The large momentum of the water near the surface of the bubble is consistent with this observation.

The late-time experimental data shown in Fig. 11 suggests that the plumes formed after collapse of the bubble may be the primary source of the large waves characteristic of the upper critical depth. B. G. Craig of GMX-8 is presently studying the long-term plume and wave behavior for the A.E.C. Tamarin committee. The results of this study may indicate where future theoretical studies should be concentrated.

ACKNOWLEDGMENTS

The radiographic study was performed by Roger London, Roger Taylor, and Douglas Venable of GMX-11. The photographic study was performed by G. B. Craig of GMX-8 and John Taylor of GMX-6. The author gratefully acknowledges the suggestions and contributions of Kenneth Olsen of J-9, James D. Kershner of T-4, Gaylord Miller of NOAA Environmental Research Laboratories, Bernard Le Mehaute of Tetra Tech, Inc., John Pritchett of Information Research Associates, and William G. Van Dorn of Scripps Institution of Oceanography.

These studies have been performed for the U. S. Atomic Energy Commission Tamarin Committee.

REFERENCES

1. Charles L. Mader, "Compressible Numerical Calculations of Underwater Detonations," Los Alamos Scientific Laboratory report LA-4594 (1971).

2. D. Venable, "PHERMEX," Physics Today 17, 19 (1964).

3. Charles L. Mader, "The Two Dimensional Hydrodynamic Hot Spot," Los Alamos Scientific Laboratory reports LA-3077 (March 1964) and LA-3235-Vol. II (Nov. 1964).

4. James D. Kershner and Charles L. Mader, "2DE: A Two Dimensional Continuous Eulerian Hydrodynamic Code for Computing Multicomponent Reactive Hydrodynamic Problems," Los Alamos Scientific Laboratory report LA-4846 (1972).

5. Charles L. Mader and James D. Kershner, "Two-Dimensional Continuous Multicomponent Eulerian Calculations of Interaction of Shocks with V Notches, Voids and Rods in Water," Los Alamos Scientific Laboratory report LA-4932 (1972).

6. John W. Pritchett, "Incompressible Calculations of Underwater Explosion Phenomena," Proc. of the Second Int. Conf. Numerical Methods in Fluid Dynamics, Lecture Notes in Physics 8, 422 (1970).

7. John W. Pritchett, "An Evaluation of Various Theoretical Models for Underwater Explosion Bubble Pulsation," Information Research Associates report IRA-TR-2-71 (1971).

8. Francis H. Harlow and Anthony A. Amsden, "A Numerical Fluid Dynamics Calculation Method for All Flow Speeds," J. of Computat. Phys. 8, 197 (1971).

9. Bernard Le Mehaute, "Theory of Explosion-Generated Water Waves," Advan. in Hydrosci. 7, 1 (1971).

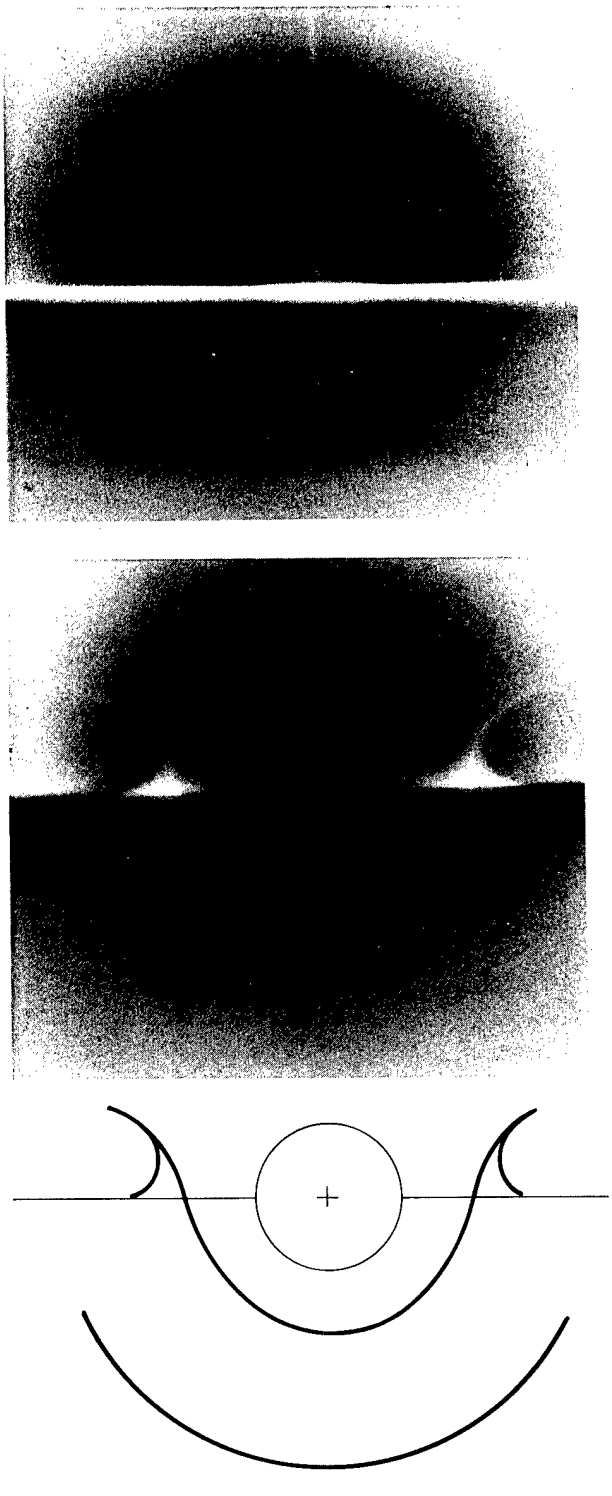

Fig. 1.
The static and dynamic radiograph at 15.8 μsec of a 1.27-cm radius explosive sphere detonating half immersed in water. A sketch of the prominent features of the radiograph is shown.

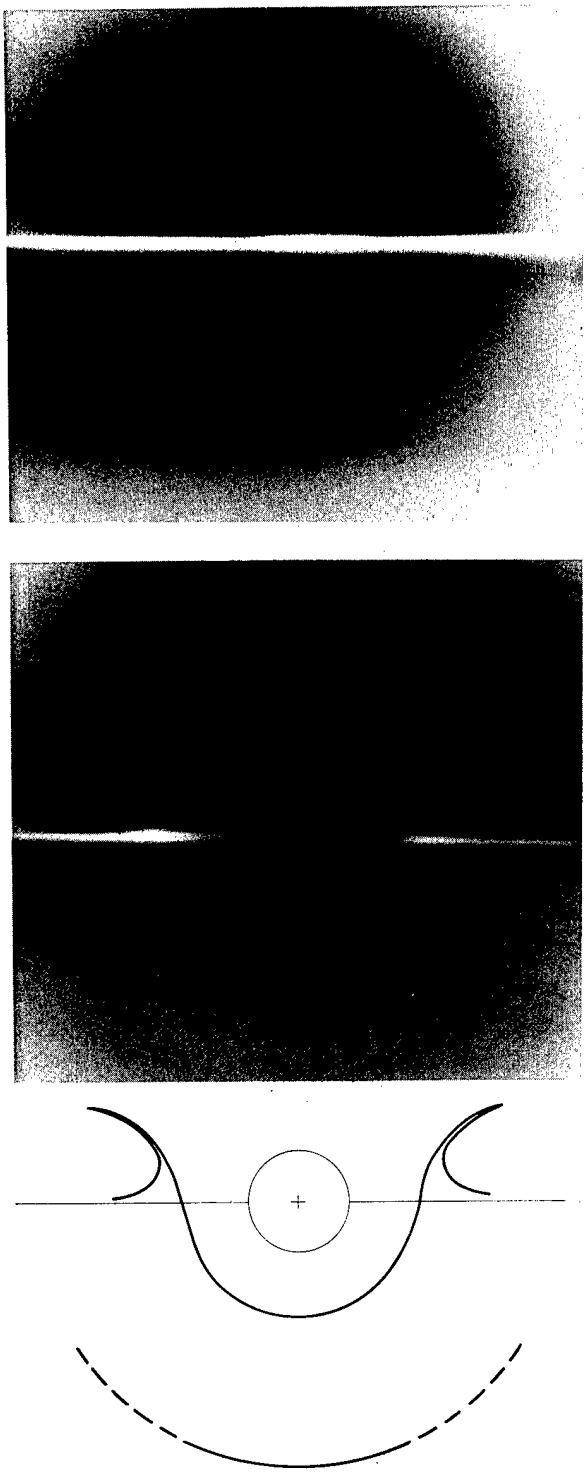

Fig. 2.
The static and dynamic radiograph at 26.3 μsec of a 1.27-cm radius sphere of 9404 detonating half immersed in water. A sketch of the prominent features of the radiographs is shown.

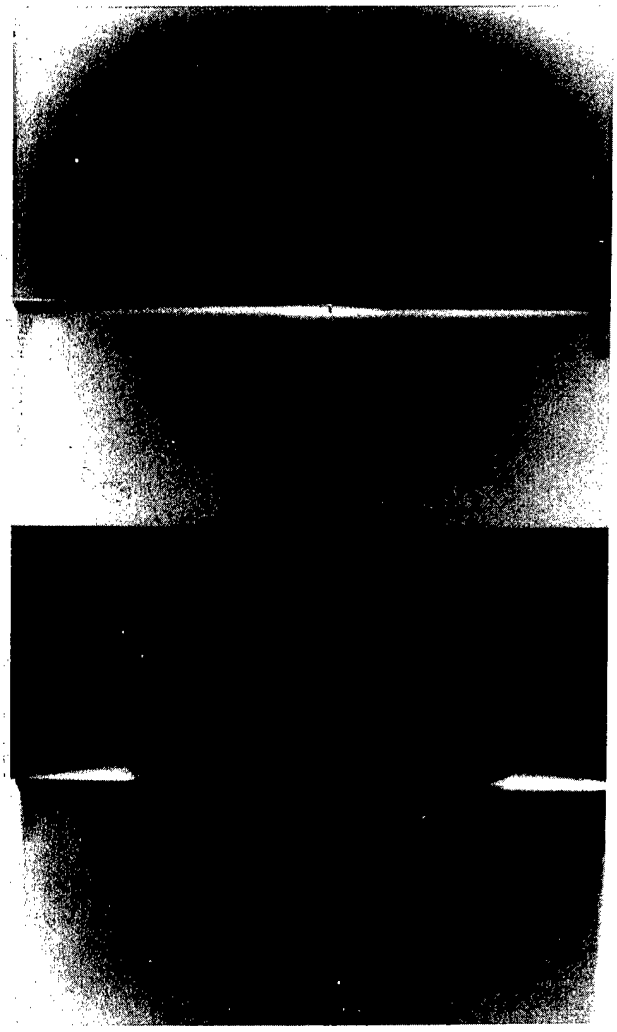

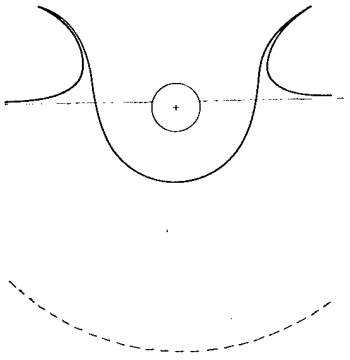

Fig. 3.

The static and dynamic radiograph at 61.3 μsec of a 1.27-cm radius sphere of 9404 detonating two-thirds immersed in water. (The dynamic radiogrphs also shows some New Mexican folk art added by the technician.) A sketch of the prominent features of the radiograph (sadly without any folk art) is shown.

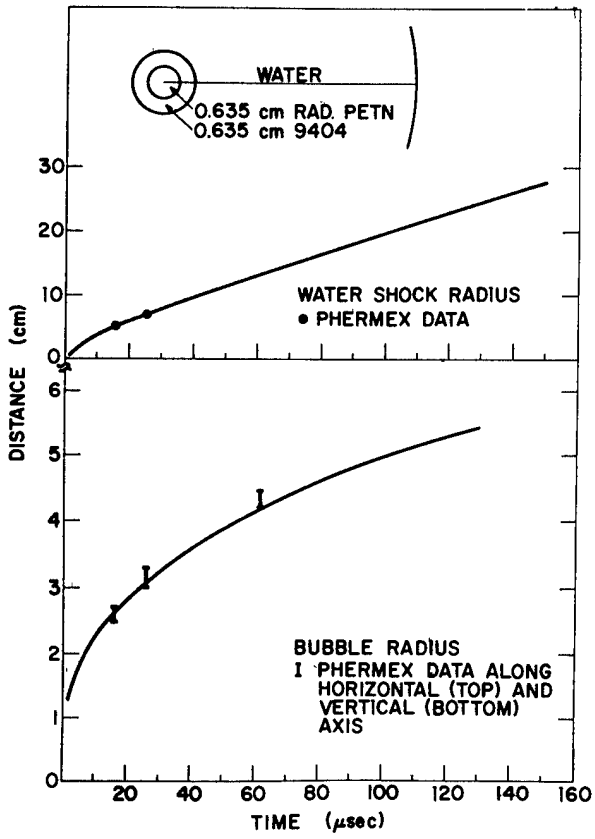

Fig. 4.

The water shock and explosive-water interface radius as a function of time for a 1.27 cm radius explosive sphere in water at 1 bar. Also shown are the positions determined from the radiographic study.

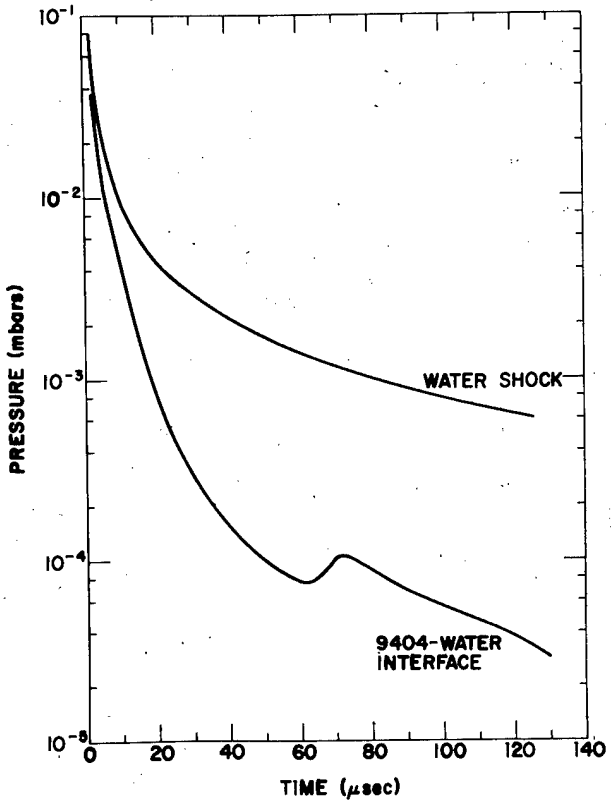

Fig. 5.
The water shock and explosive-water interface pressure as a function of time for a 1.27-cm radius explosive sphere in water at 1 bar.

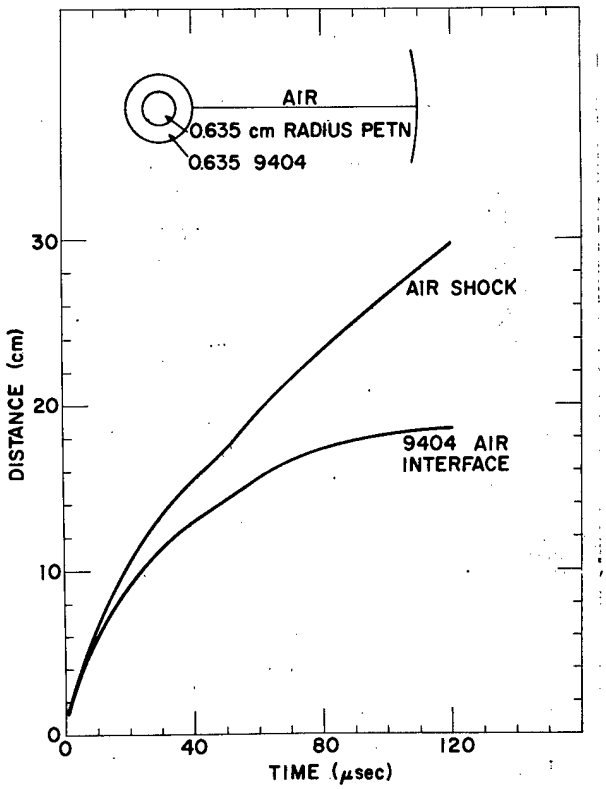

Fig. 6.
The air shock and explosive-air interface radius as a function of time for a 1.27-cm radius explosive sphere in air at one Los Alamos atmosphere.

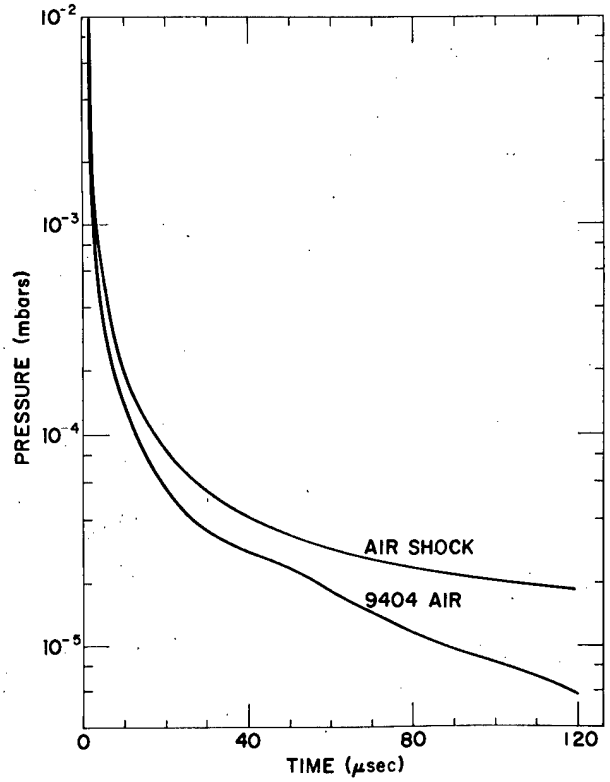

Fig. 7.
The air shock and explosive air interface pressure as a function of time for a 1.27-cm radius explosive sphere in air at one Los Alamos atmosphere.

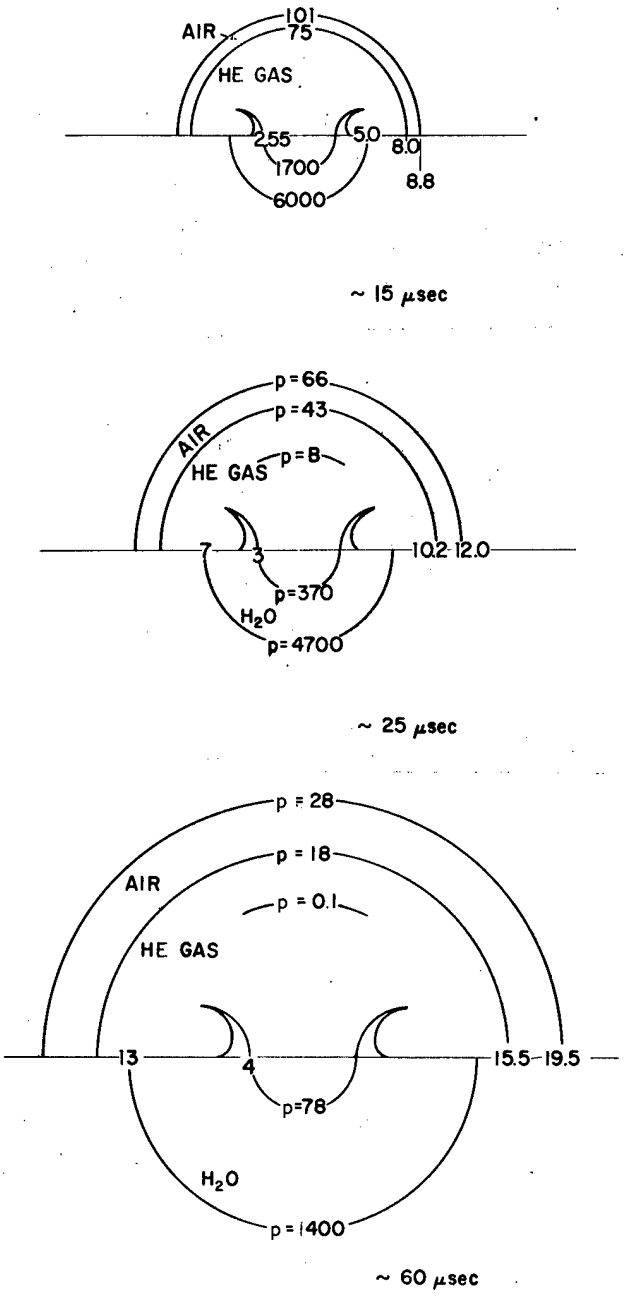

Fig. 8.
Sketches of the important features of the flow of a 1.27-cm radius explosive sphere interacting with a water-air interface at the times used in the radiographic study. The calculated one-dimensional pressures in bars and positions of the air shock and air-detonation-product interface in centimeters are shown along the vertical axis.

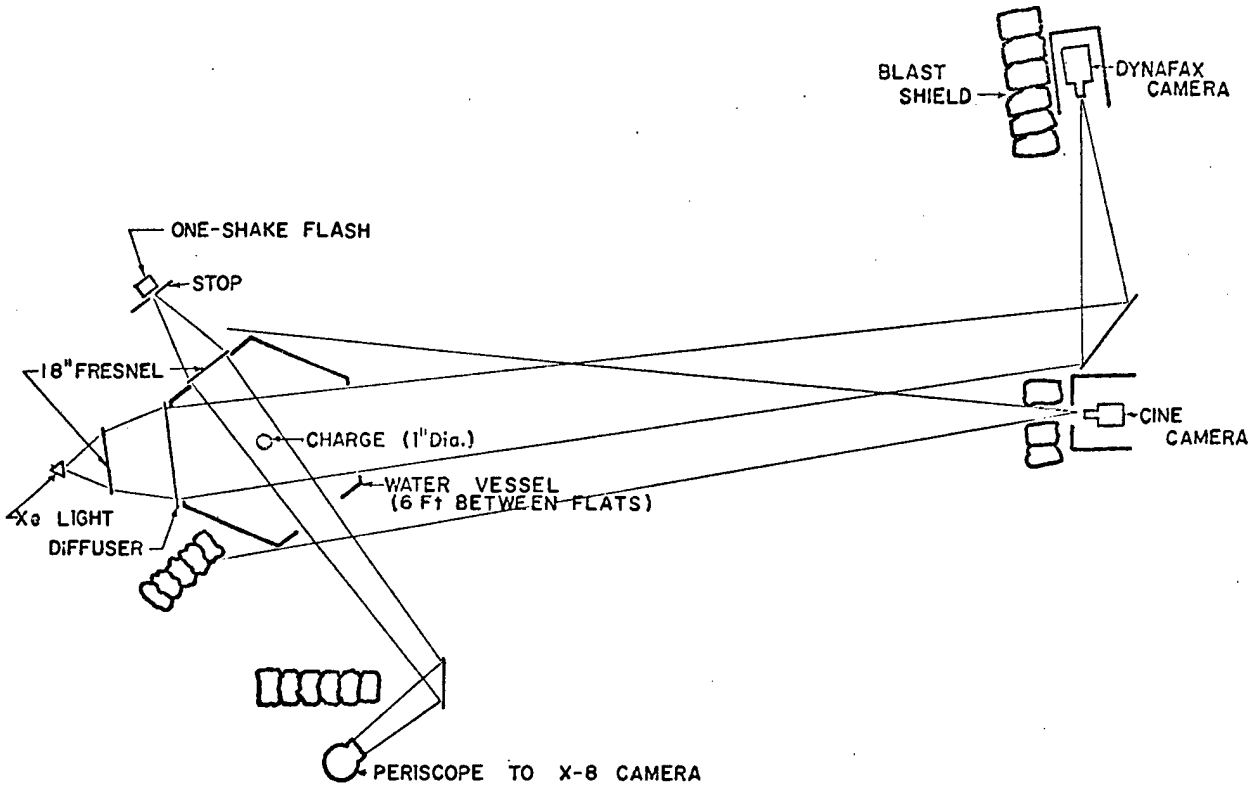

Fig. 9.
The experimental arrangement for the photographic study.

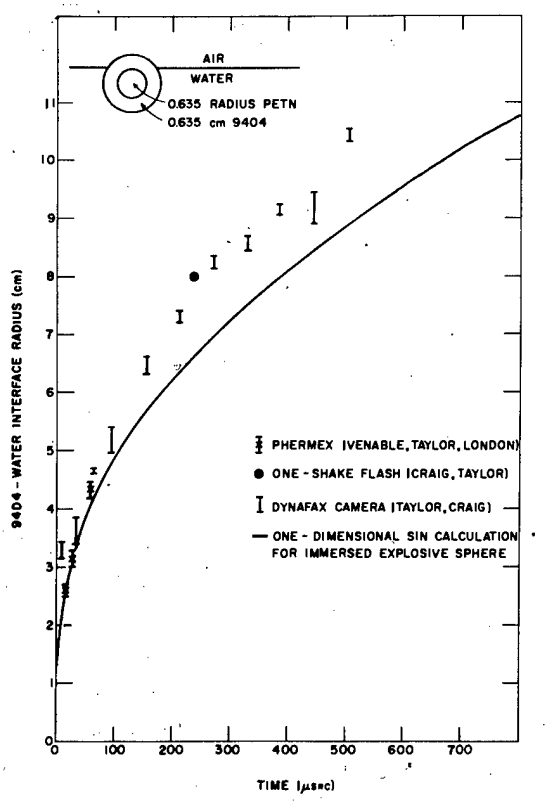

Fig. 10.
The detonation product-water radius calculated using the one-dimensional model and the experimental data as a function of time. The experimental data is shown with a bar whose top is the horizontal radius and bottom is the vertical radius through the initial center of the explosive charge.

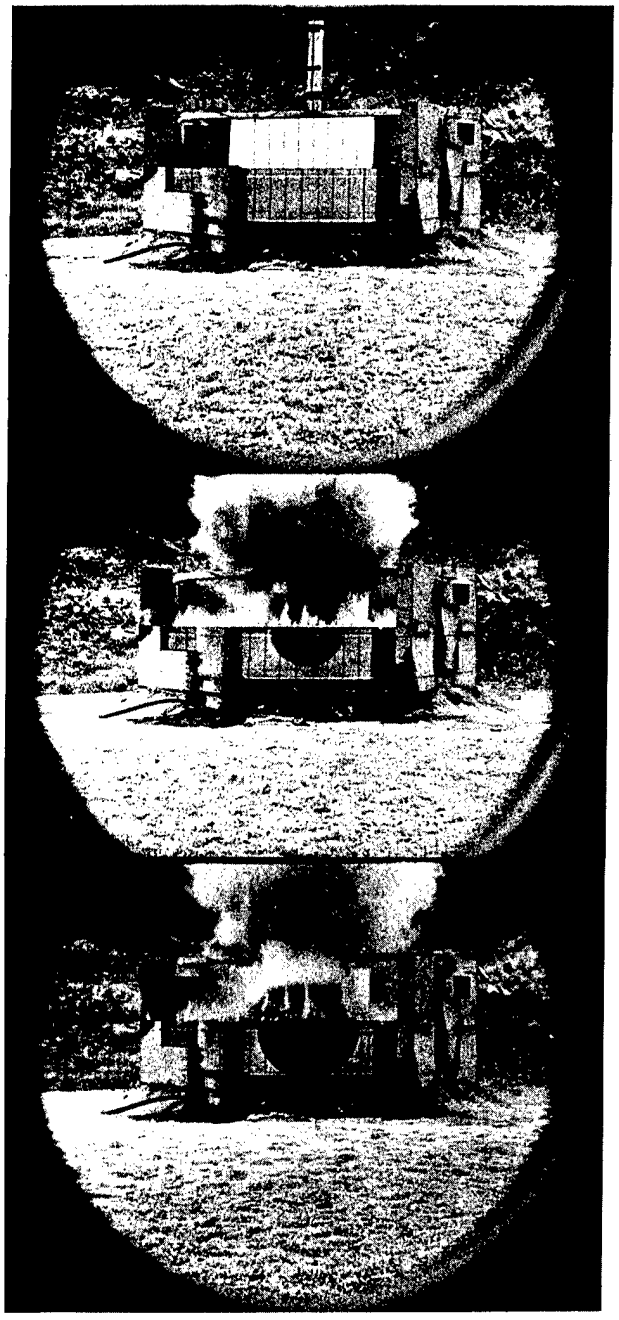

Fig. 11.
Selected frames from the cine camera data. The time between frames was 0.0156 seconds, the exposure time was 0.002 seconds per frame. The grid behind the shot was 4 in. between lines.

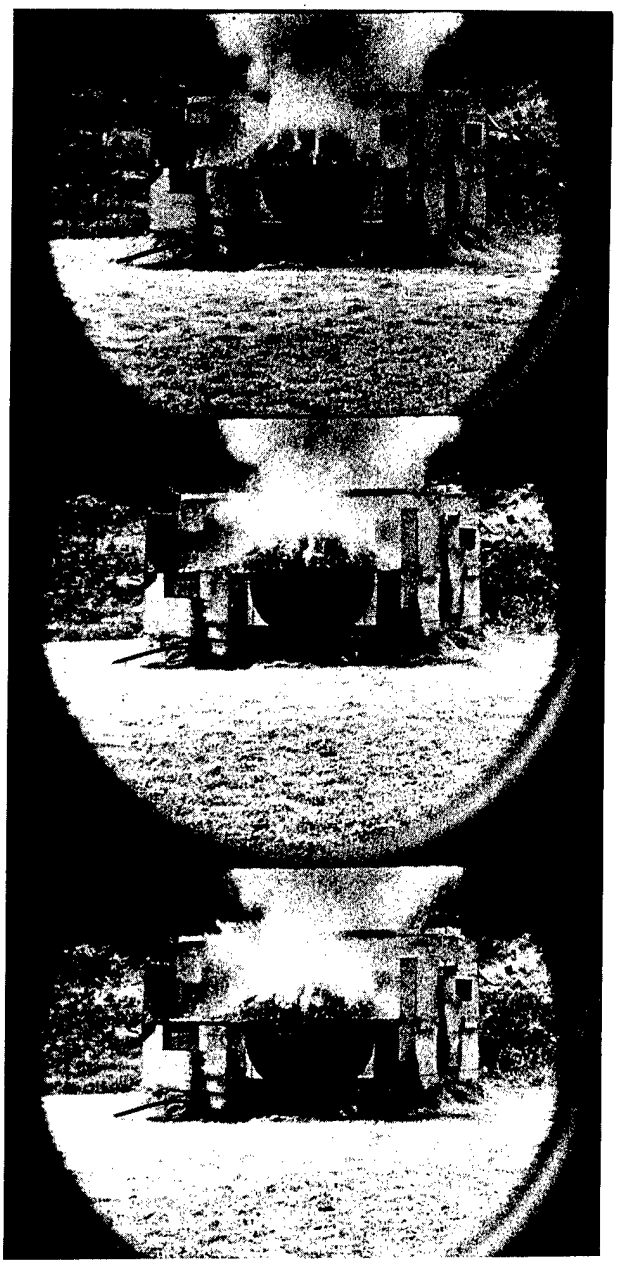

Fig. 11. (cont)

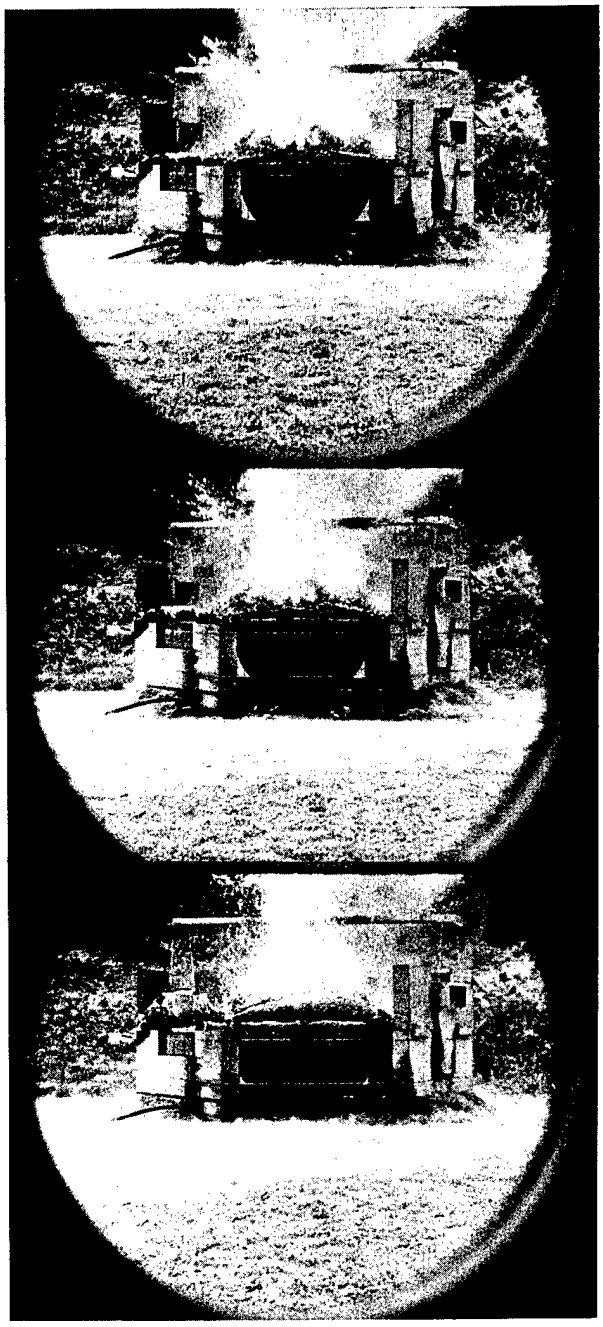

Fig. 11. (cont)

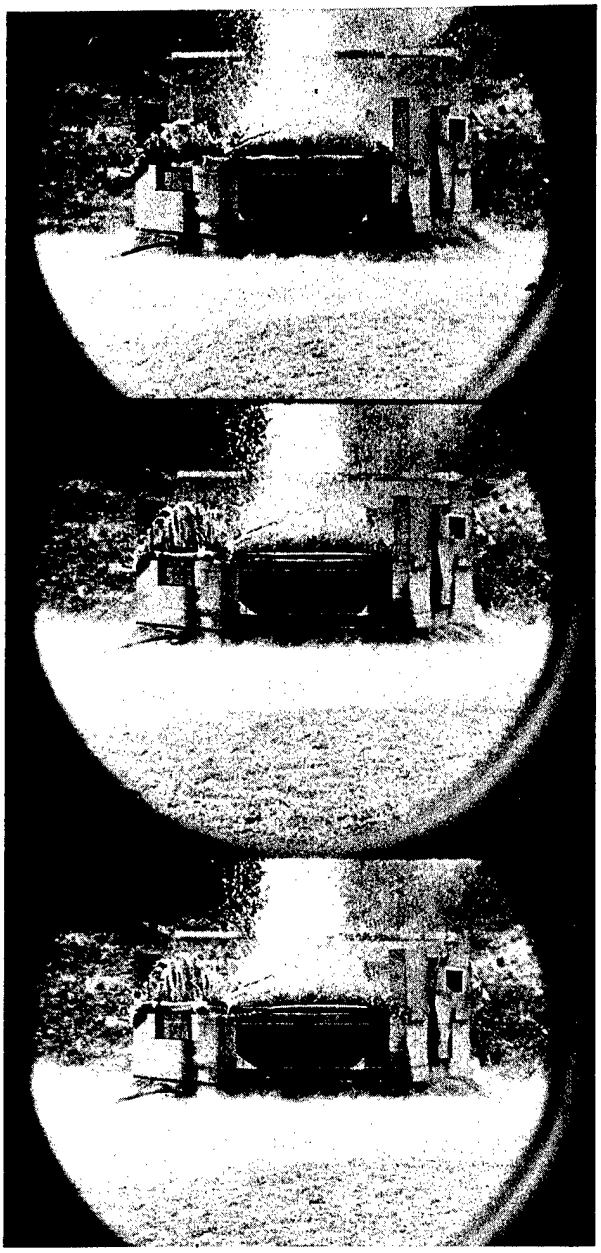

Fig. 11. (cont)

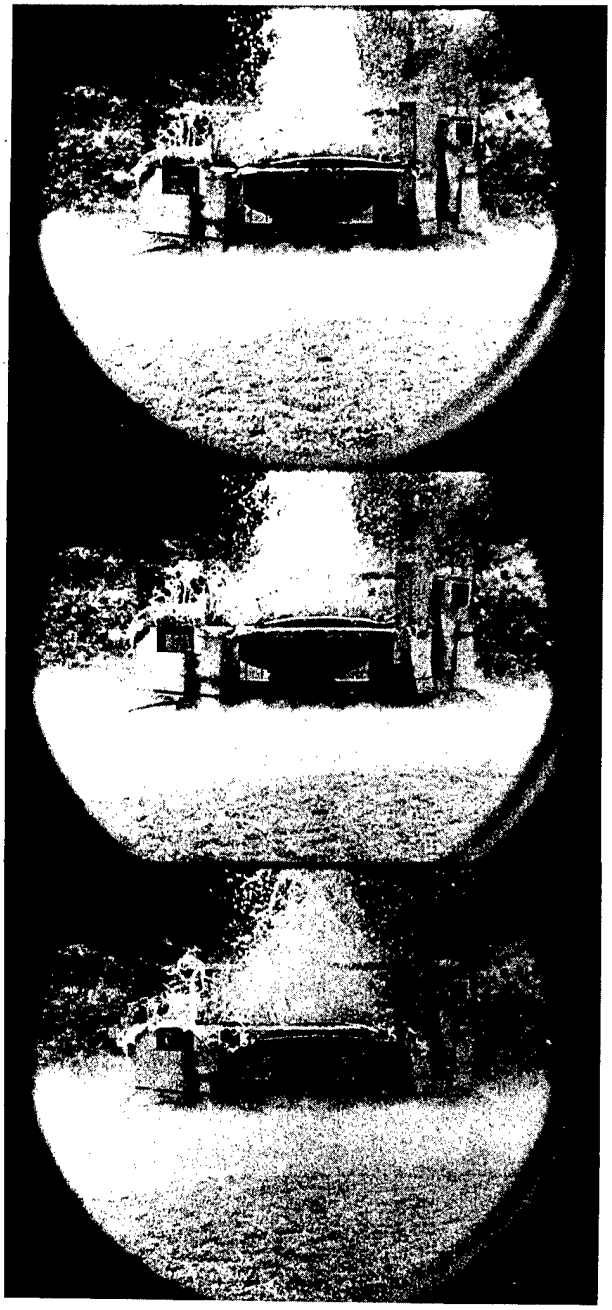

Fig. 11. (cont)

Fig. 11. (cont)

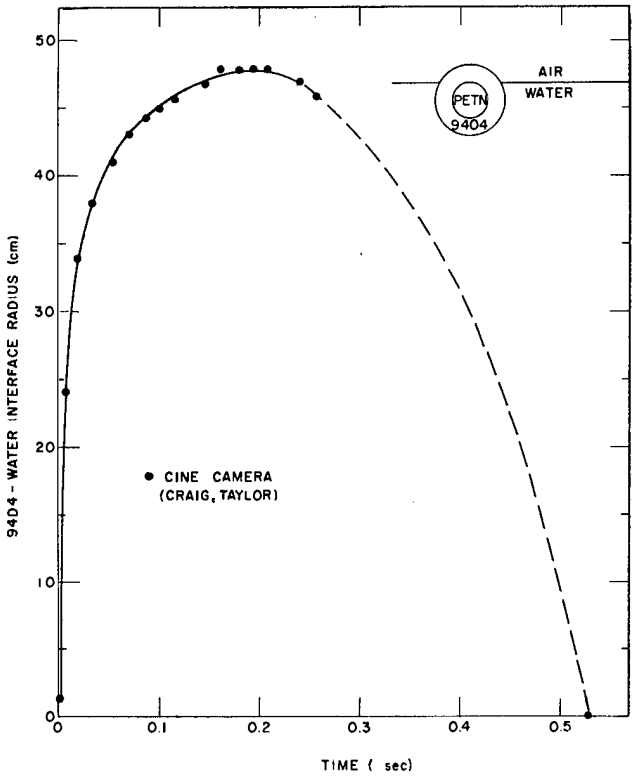

Fig. 12.
Preliminary cine camera data of the detonation product-water radius as a function of time.

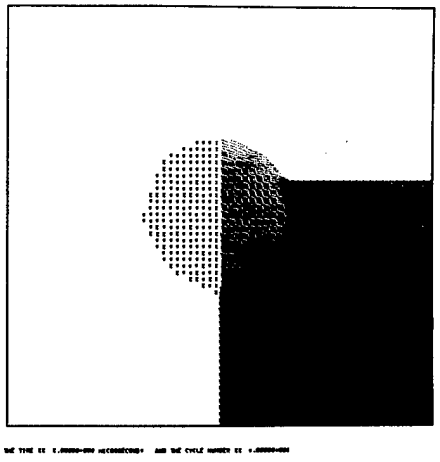

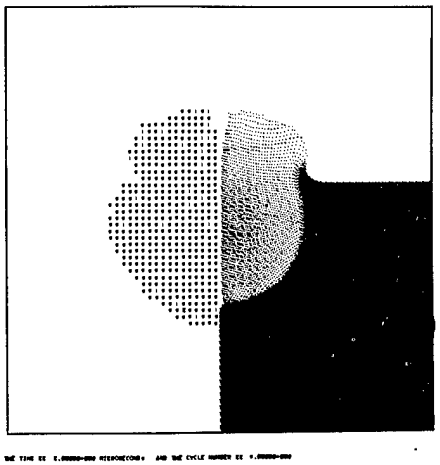

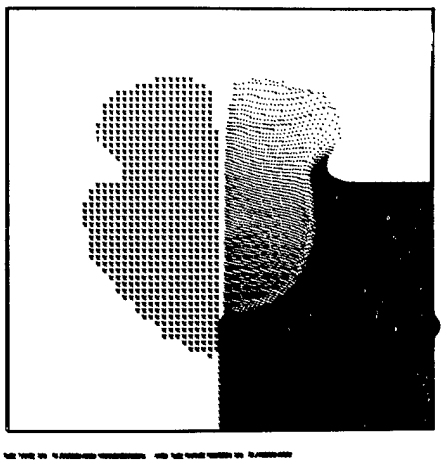

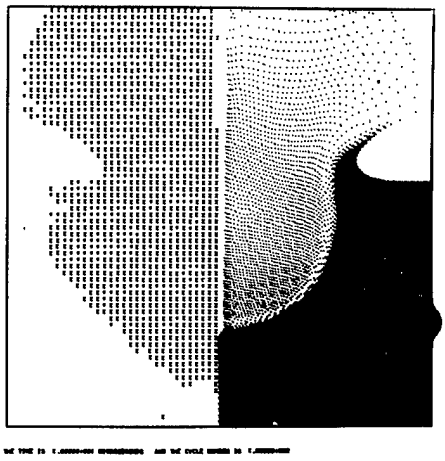

Fig. 13.
PIC (Particle-In-Cell) calculations of a 1.27-cm radius sphere of 9404 initiated at its center and immersed in water at various levels. The "X" plotting symbols on the left indicate the position of cells that have been shocked to temperatures greater than ambient.

Fig. 13. (cont)

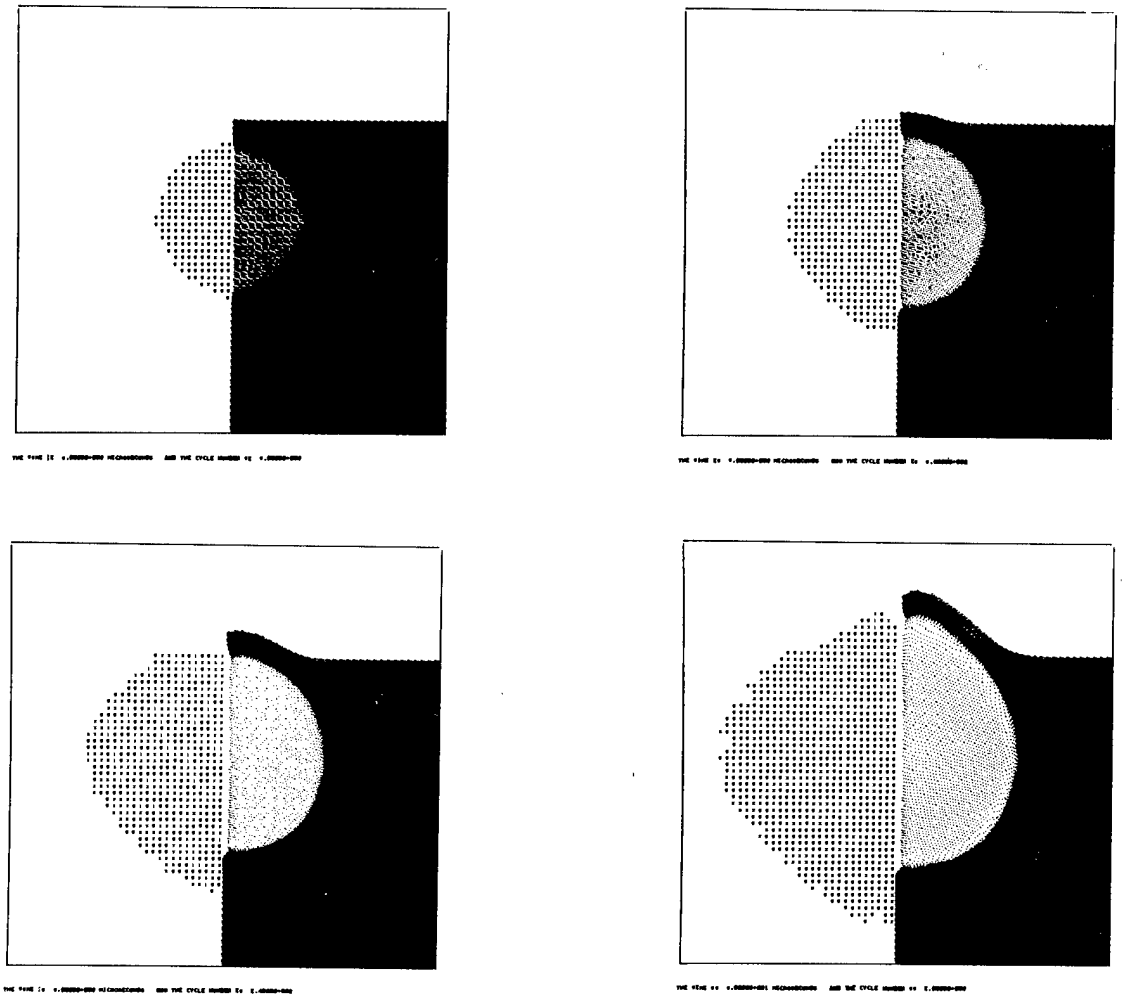

Fig. 13. (cont)

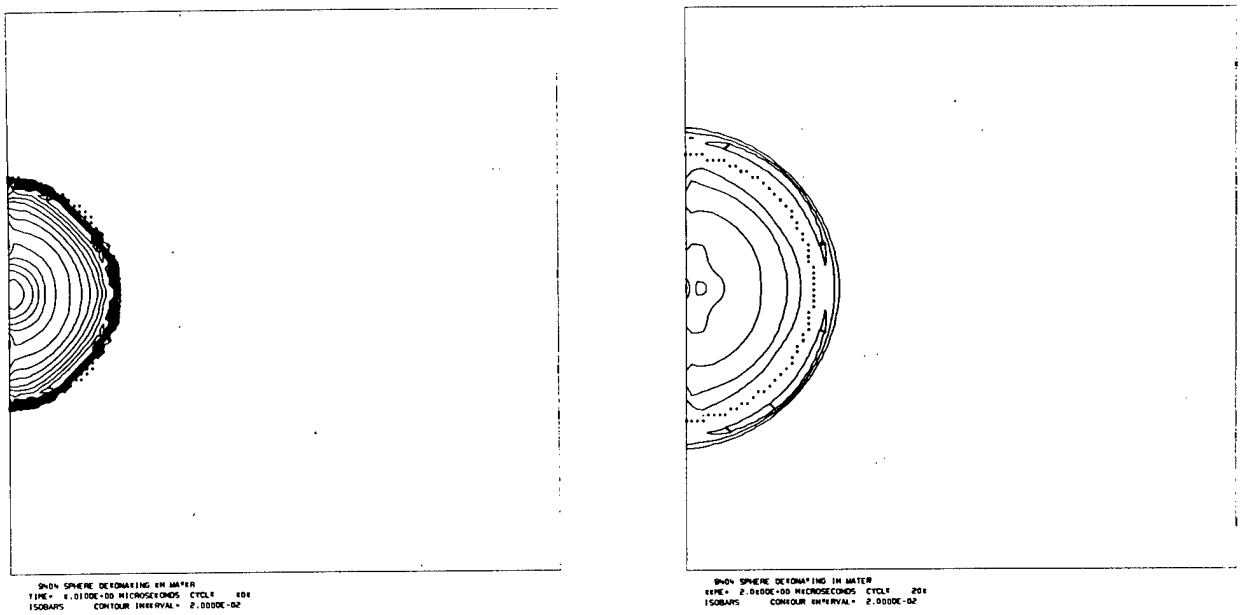

Pressure

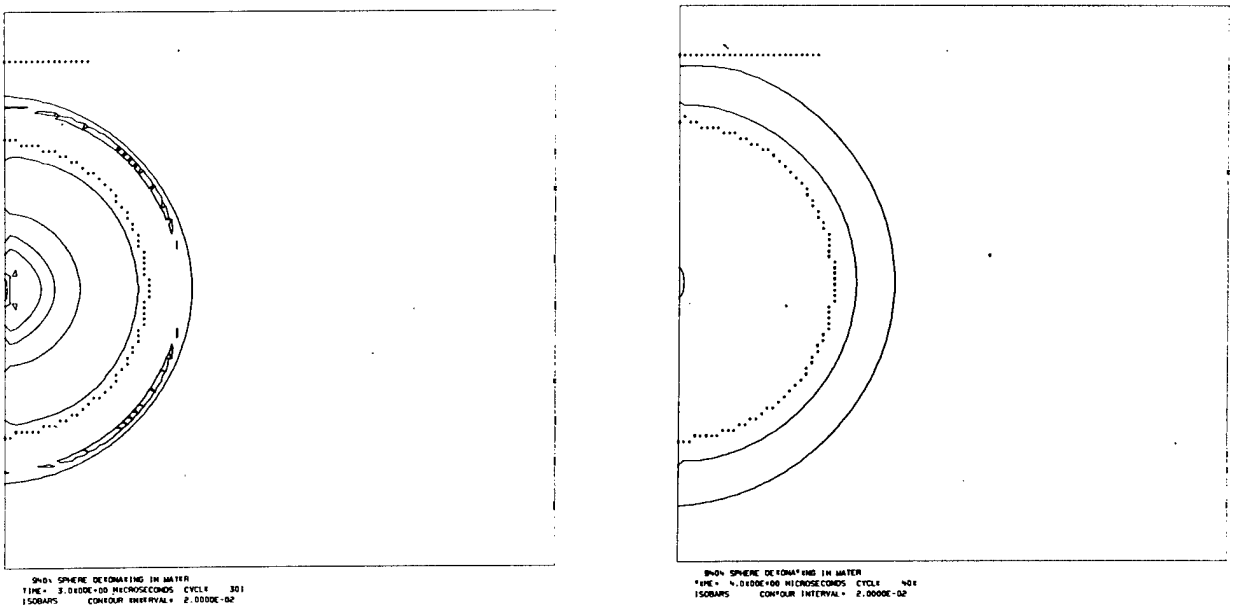

Fig. 14.
Two-dimensional Eulerian calculations of a 1.27-cm radius 9404 sphere initiated at its center by a 0.4-cm radius initiator and immersed under 1.27-cm of water. The pressure contour interval is 20 kbars, the density contour interval is 0.2 gm/cc, and the velocity contour interval is 0.05 cm/μsec. The position of mixed cells (9404-water, 9404-air, water-air or 9404-water-air) is shown with an "X" plotting symbol.

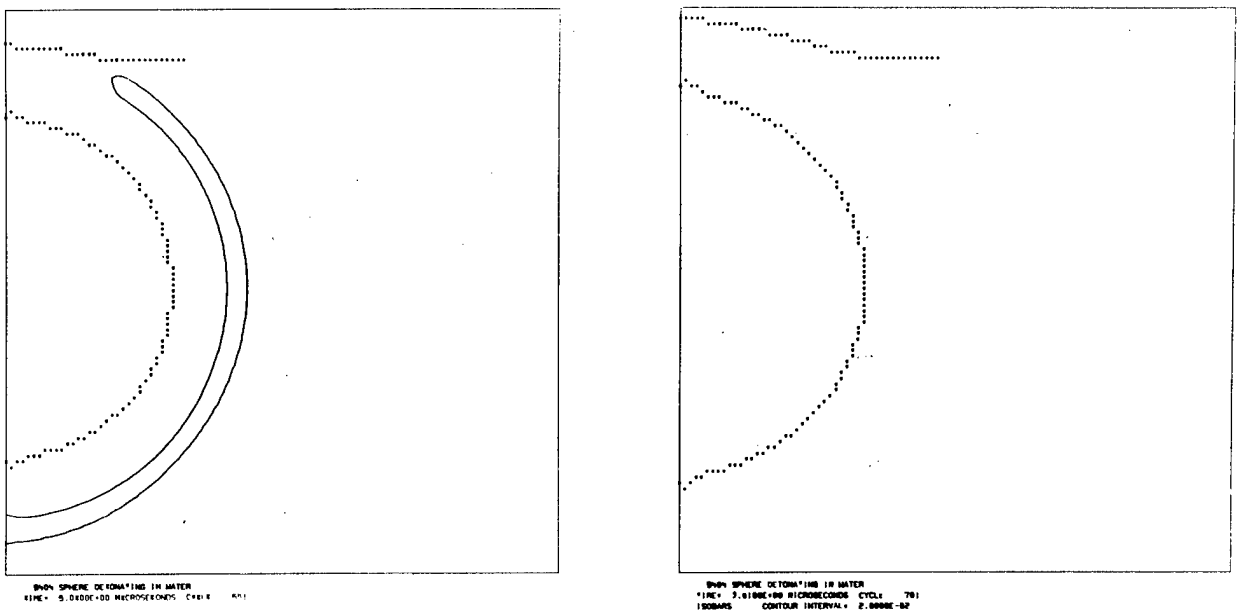

pressure

Fig. 14. (cont)

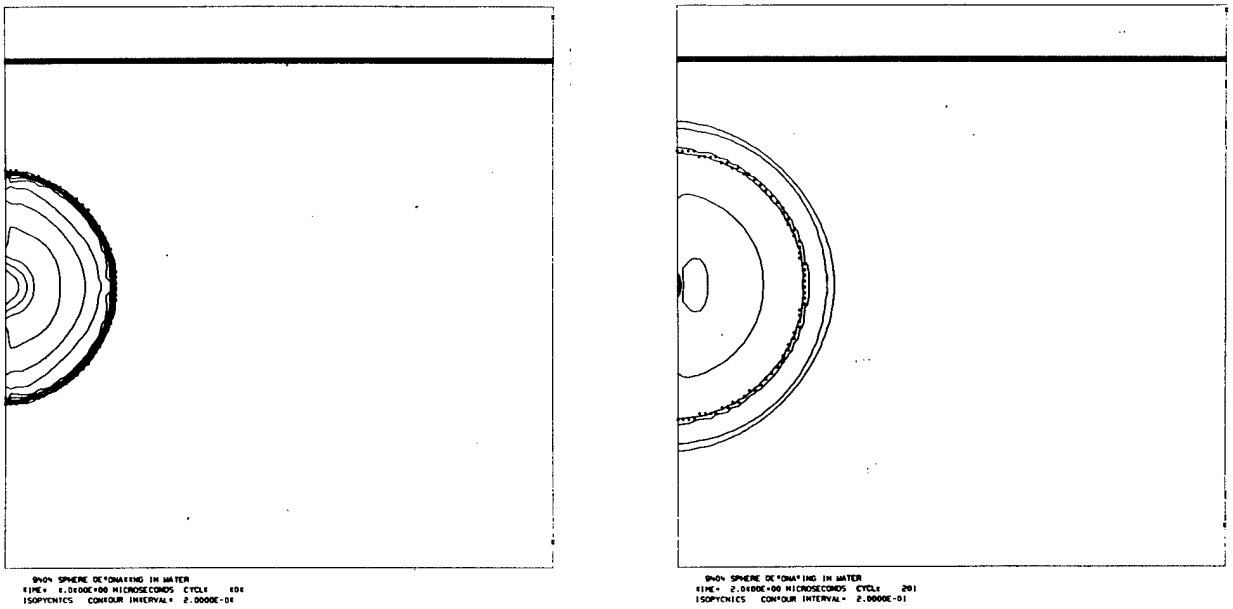

density

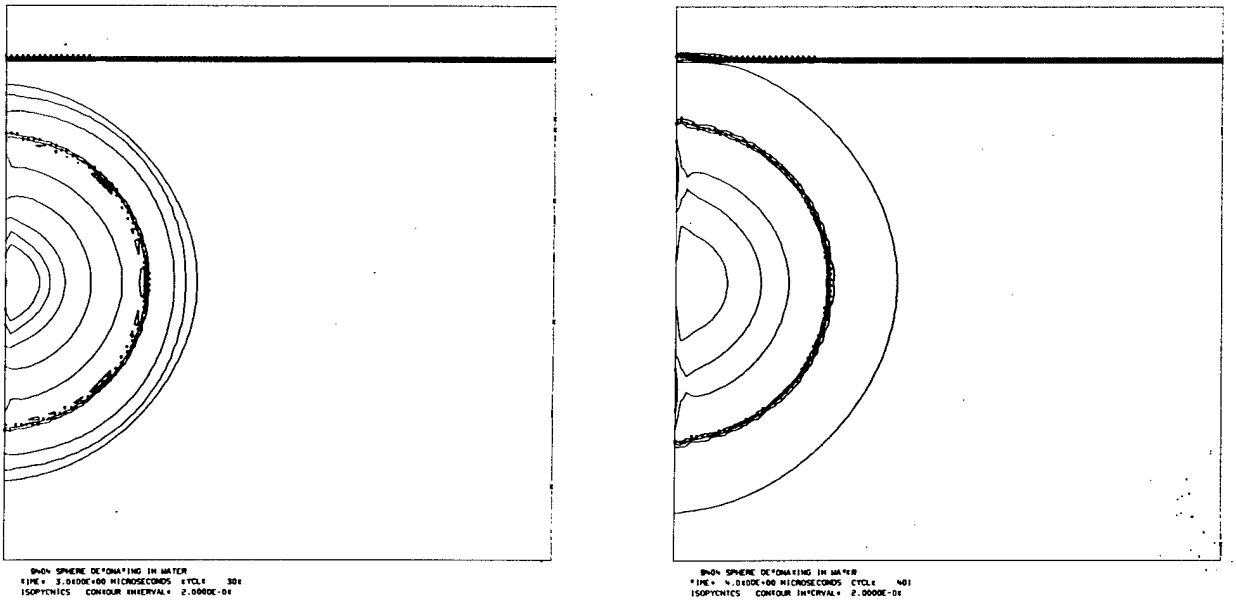

Fig. 14. (cont)

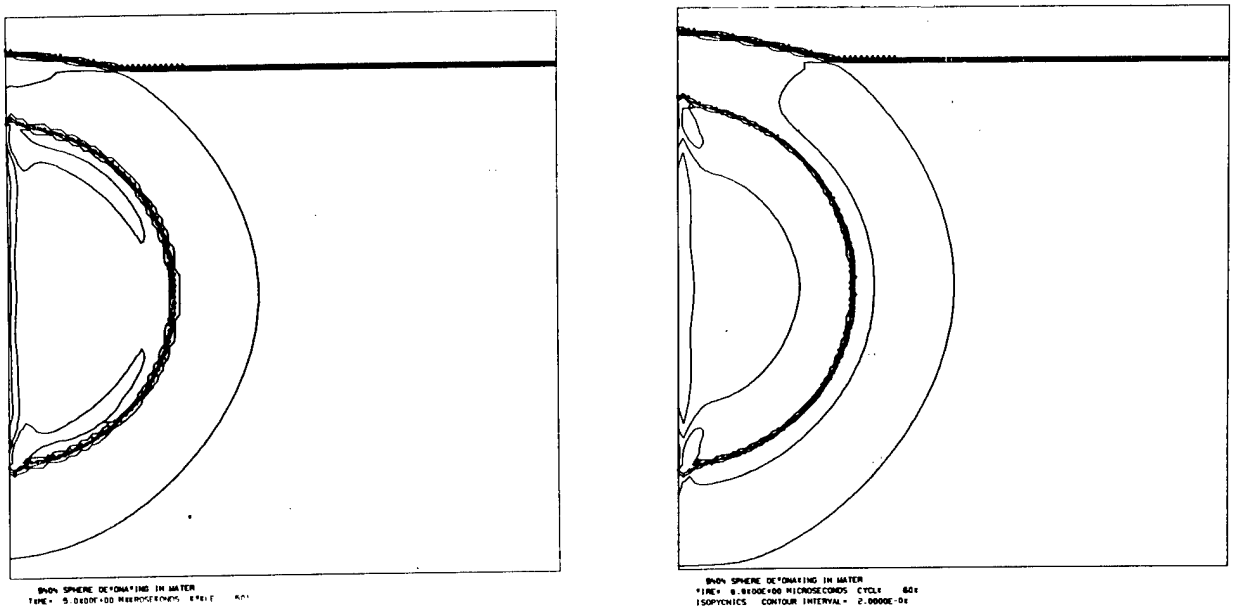

density

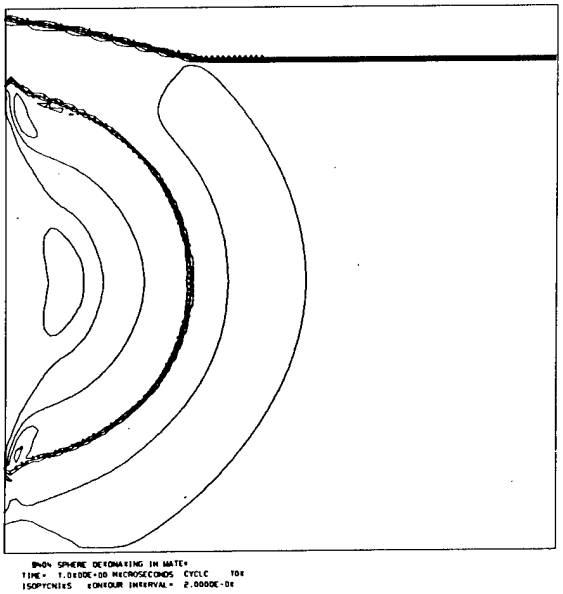

Fig. 14. (cont)

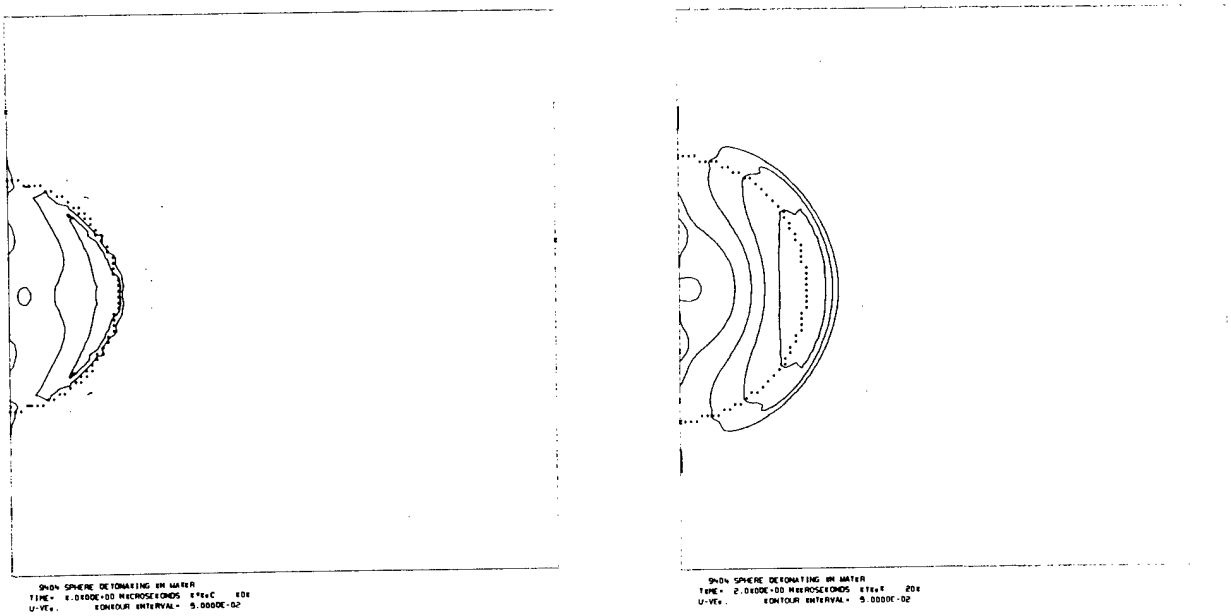

Velocity in R direction

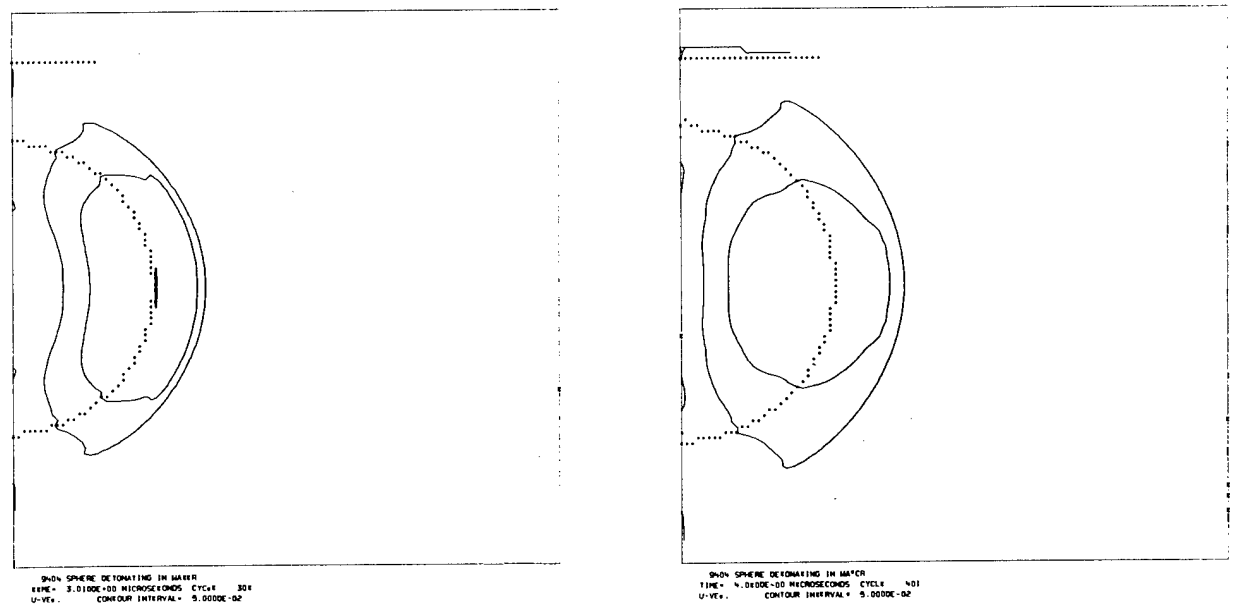

Fig. 14. (cont)

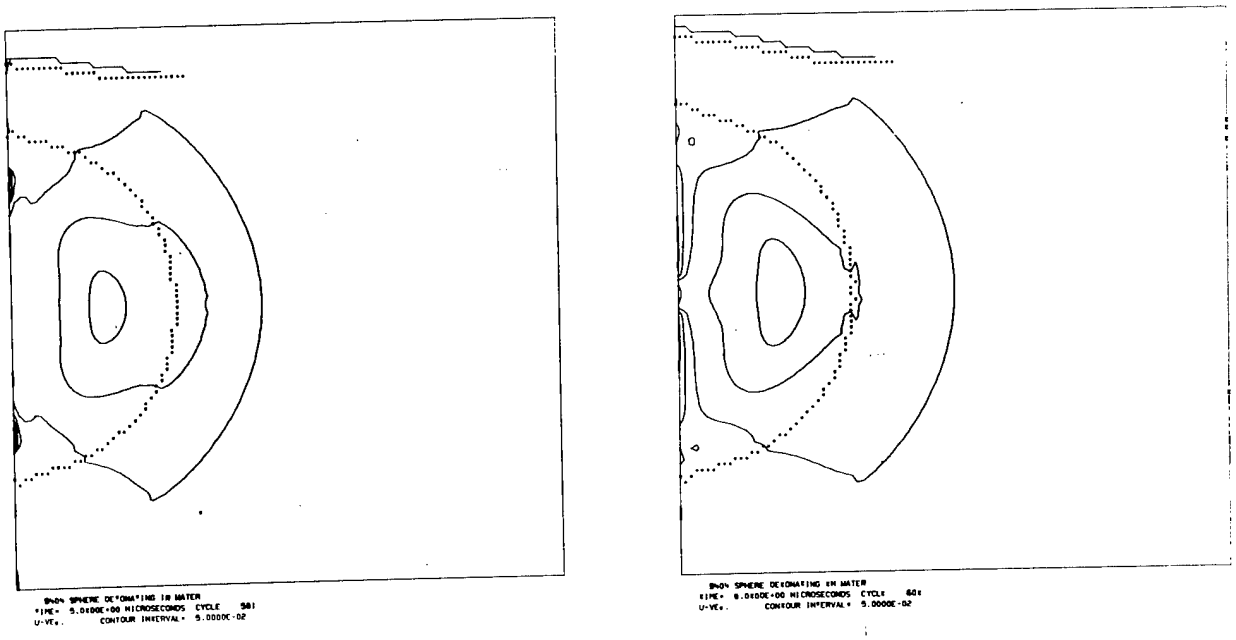

Velocity in R direction

Fig. 14. (cont)

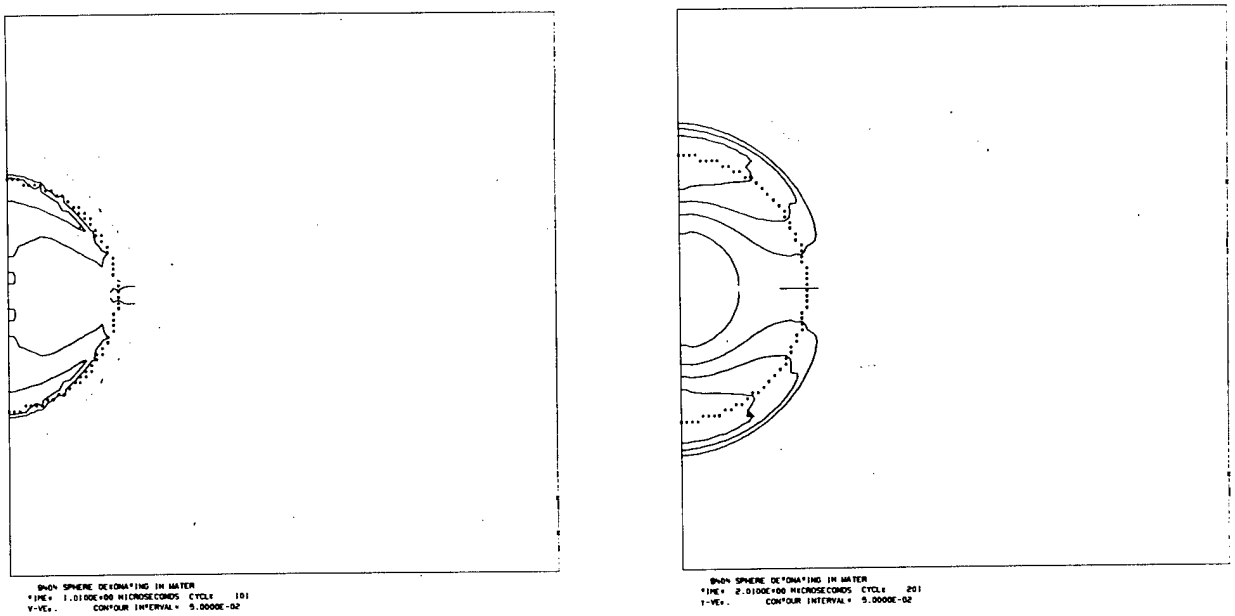

Velocity in Z direction

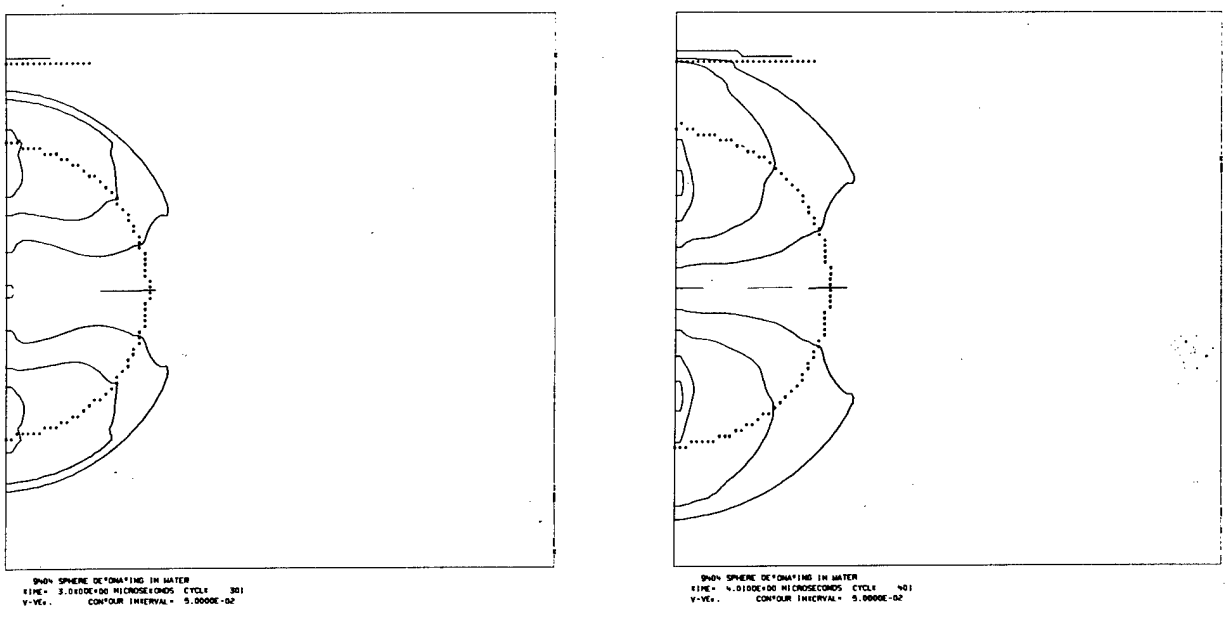

Fig. 14. (cont)

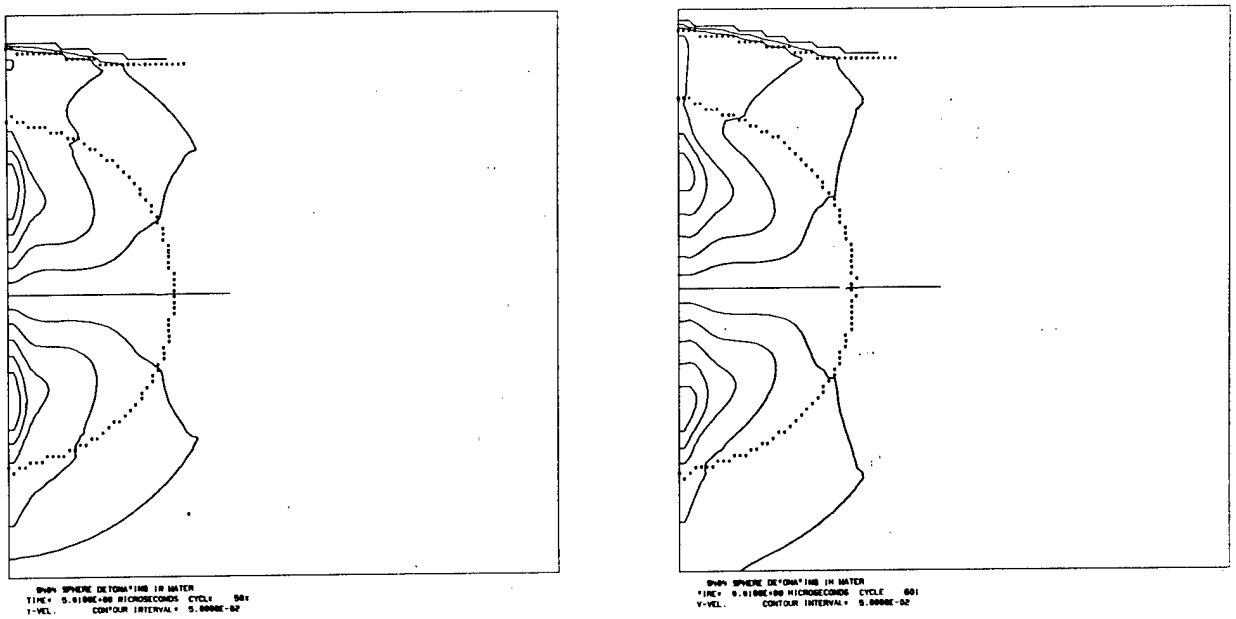

Velocity in Z direction

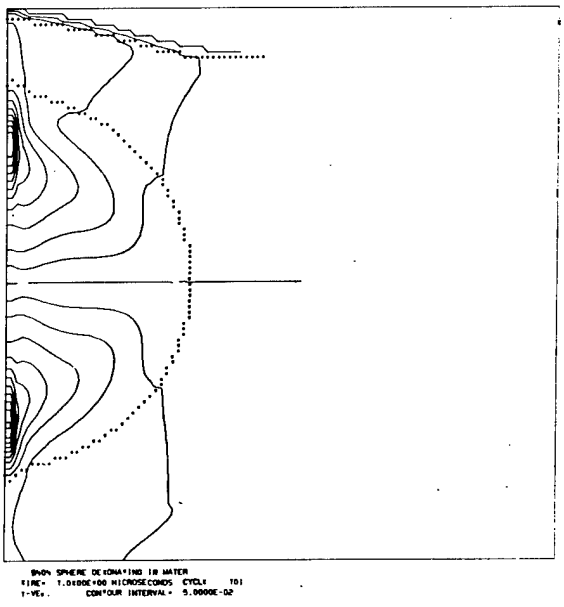

Fig. 14. (cont)

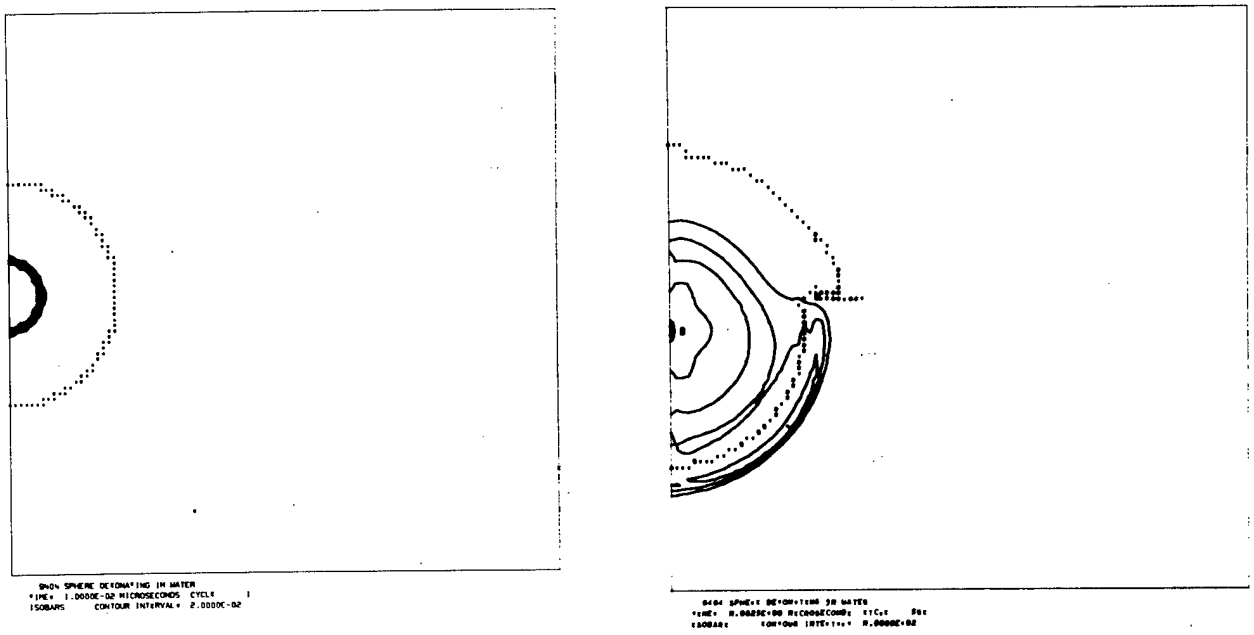

pressure

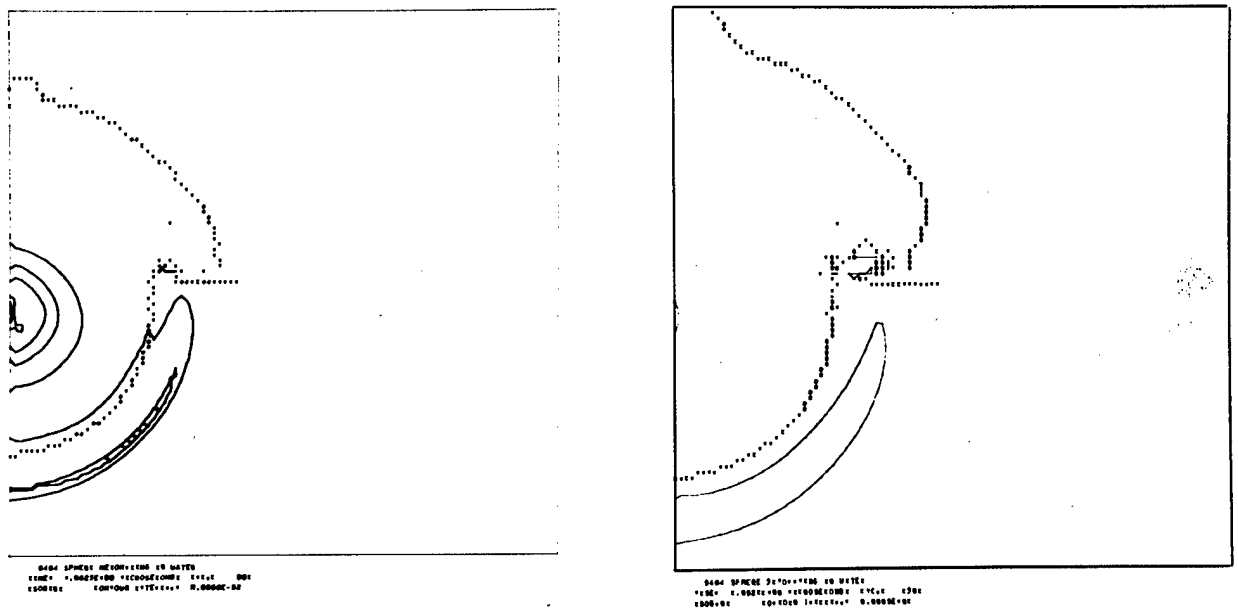

Fig. 15.
Two-dimensional Eulerian calculations of a 1.27-cm radius 9404 sphere initiated at its center by a 0.4-cm radius initiator and immersed to a depth of 1.5875 cm. The contour intervals are the same as Fig. 14.

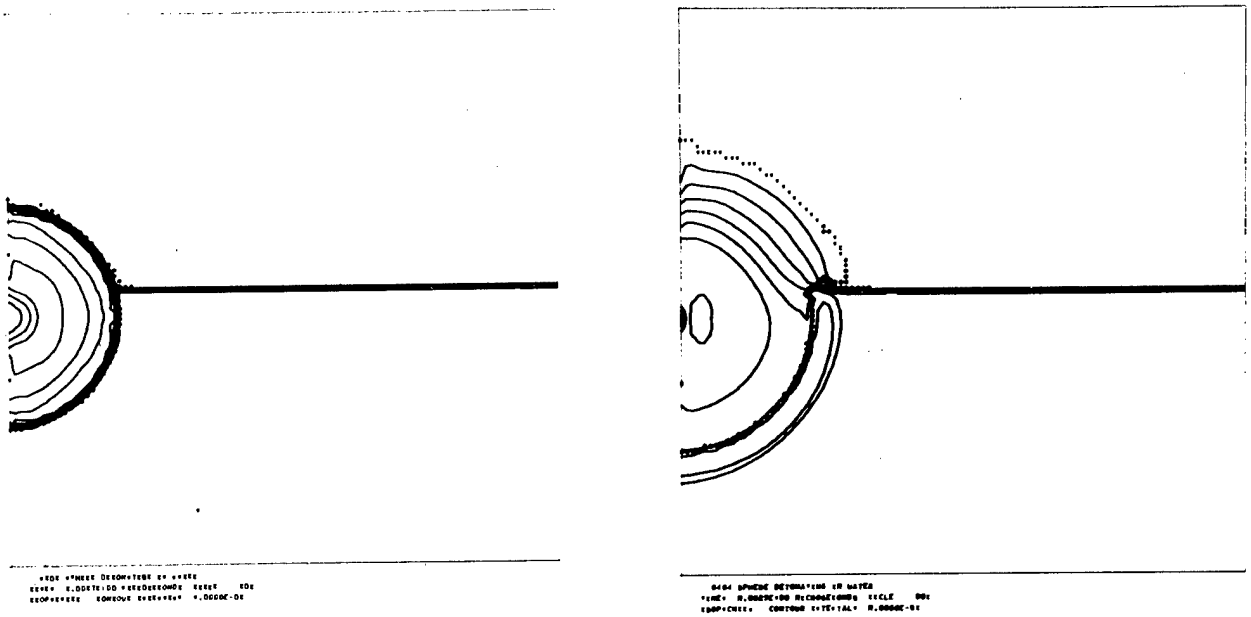

density

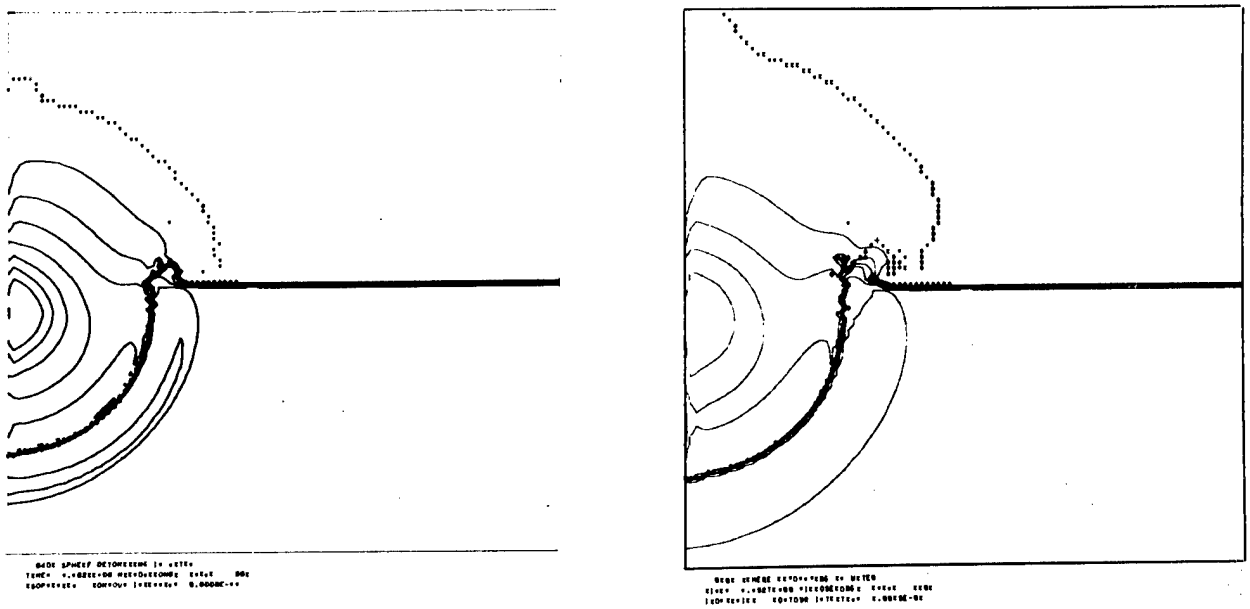

Fig. 15. (cont)

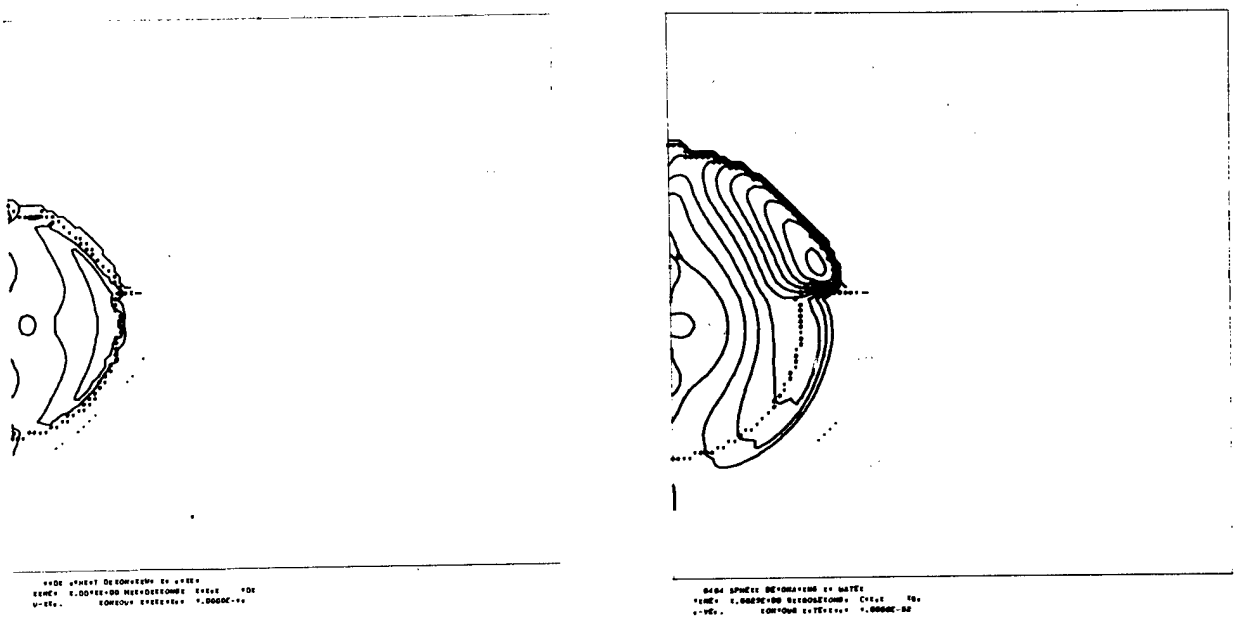

velocity in R direction

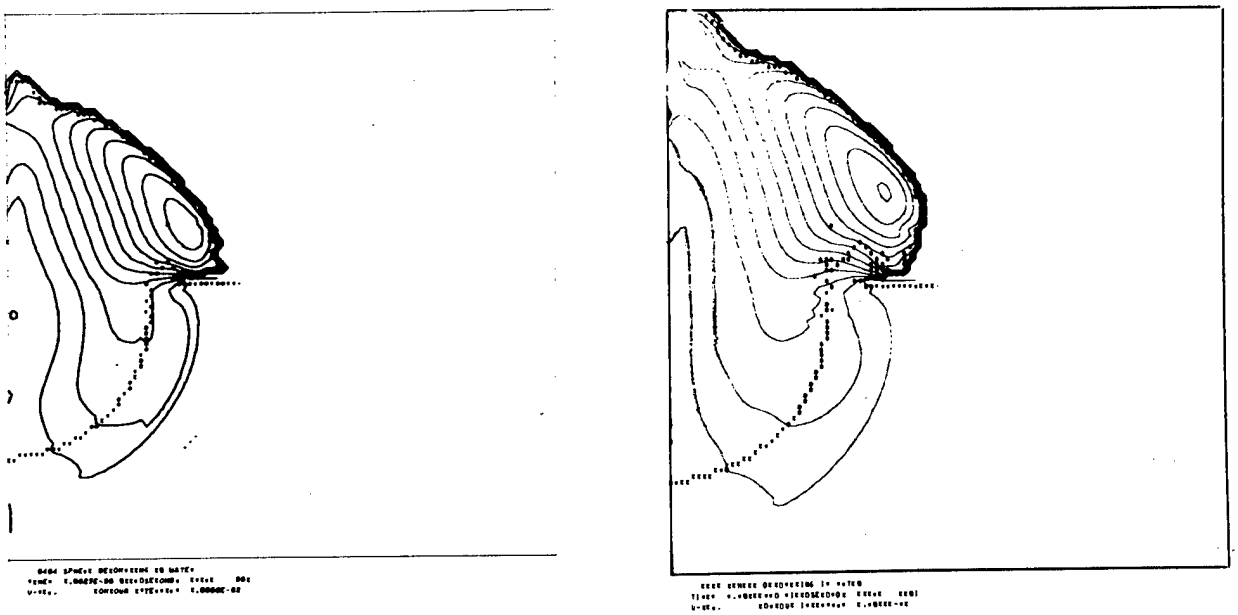

Fig. 15. (cont)

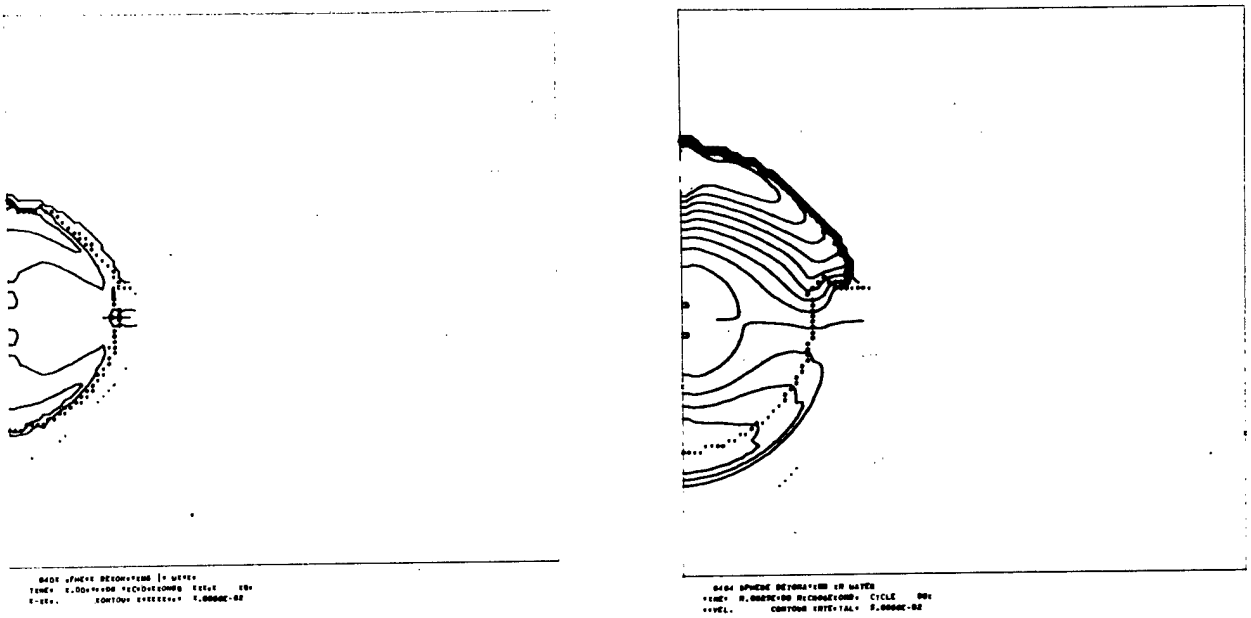

velocity in Z direction

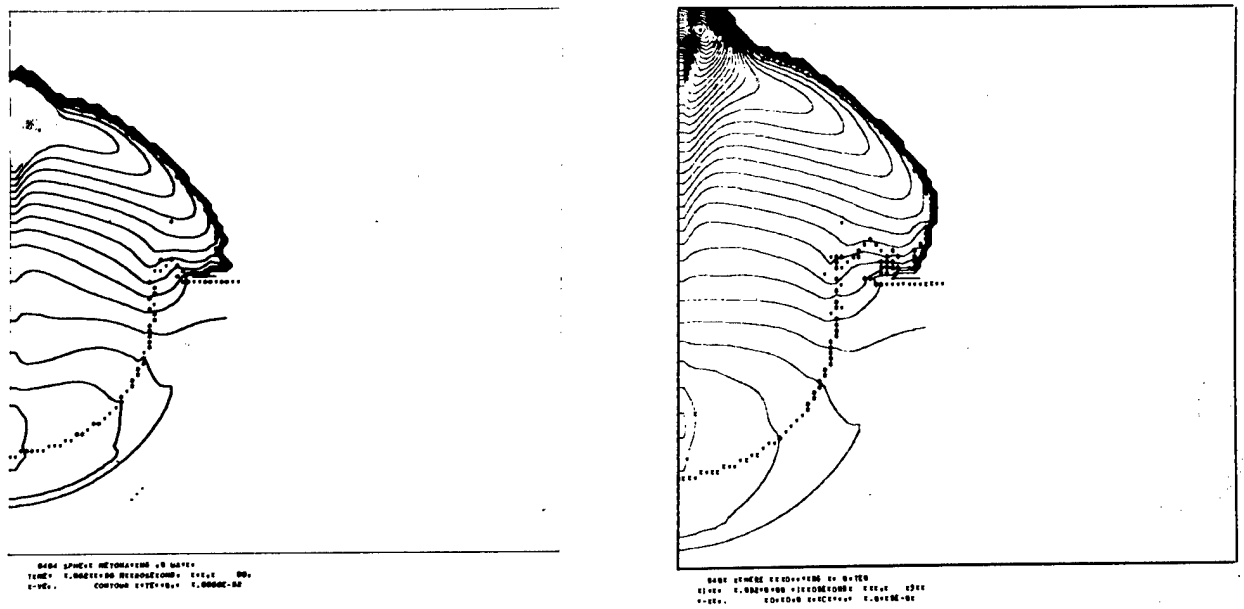

Fig. 15. (cont)

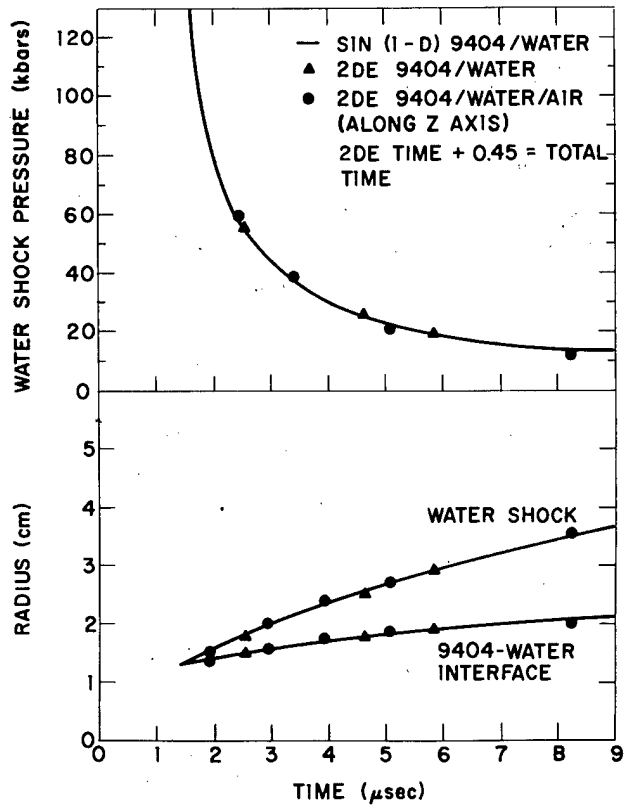

Fig. 16.
Calculated position of the water shock, 9404-water interface and water shock pressure as a function of time for the SIN and 2DE calculations.

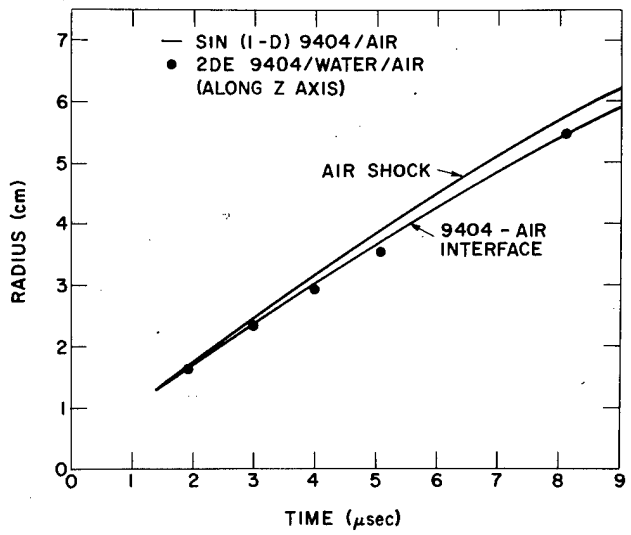

Fig. 17.
Calculated position of the air shock and the 9404-air interface as a function of time for the SIN and 2DE calculations.

CM/je:475(200)